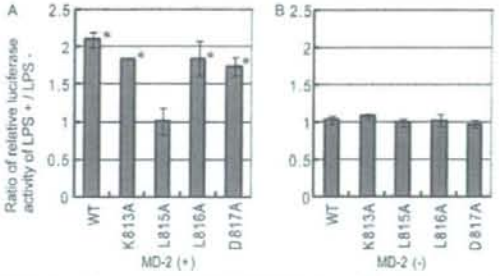

FIGURE 6. **Leucine at position 815 of TLR4 is pivotal for LPS responsiveness as measured by NF-κB luciferase assay.** *A*, HEK293T cells were transfected with single amino acid replacement mutants of the human TLR4-EGFP fusion protein plasmid, human MD-2 plasmid, and luciferase reporter and control plasmids. After 36 h, cells were stimulated with LPS (10 ng/ml) for 7 h, and luciferase reporter gene activity was measured. *B*, instead of MD-2, an empty vector was cotransfected with TLR4-EGFP plasmid and reporter assay vectors. LPS stimulation was done as in *A*. All results were expressed in the ratio of relative luciferase activity with LPS stimulation to that without the stimulation as in Fig. 2. The data were from three independent experiments. *Small bars* indicate 95% confidence intervals of the mean (*p* values for * are: TLR4 (WT)-EGFP/MD-2 (+), $p = 0.002$; TLR4 (K813A)-EGFP/MD-2 (+), $p = 0.000$; TLR4 (L816A)-EGFP/MD-2 (+), $p = 0.018$; and TLR4 (D817A)-EGFP/MD-2 (+), $p = 0.007$).

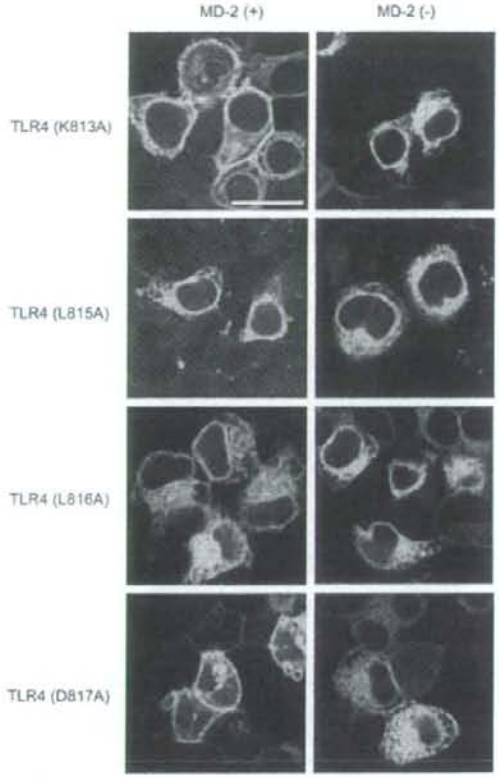

FIGURE 7. **Leucines at the position 815 and 816 of TLR4 are responsible for full plasma membrane expression.** Cells were cultured on coverslips in 12-well plates and transfected as in Fig. 2. EGFP-tagged TLR4 was visualized by laser confocal microscopy. Each genotype of TLR4-EGFP was cotransfected with human MD-2 plasmid or empty vector. *Bar*, 20 μm.

between EGFP-tagged proteins and FLAG-His_6-tagged proteins in the relative pattern of responsiveness against LPS stimulation (Fig. 8*A*). Because CD14 is also important for LPS recognition by TLR4, we examined the effect of CD14 coexpression on the phenotypic changes of the mutants (17, 18). Coexpression of CD14 did not change the phenotypes of wild-type TLR4, TLR4 (L815A), and TLR4 (L816A) in terms of LSP responsiveness (data not shown).

Cell surface expressions of the wild-type, L815A mutant, and L816A mutant TLR4-FLAG- His_6 fusion proteins were also examined. Live cells transfected with wild-type TLR4, the L815A mutant or the L816A mutant as well as human MD-2 and CD14 were biotinylated on the cell surface, and the biotinylated proteins were affinity-purified and subjected to Western blotting. Fig. 8*B* shows the marked difference in cell surface expression of wild-type and mutants L815A and L816A. Note that biotinylated proteins have additional residues on every amine of the extracellular domain, which leads to a band shift during electrophoresis. Although both mutants were detected far less than the wild-type on the cell surface, comparatively more L816A mutant was expressed on the plasma membrane than L815A mutant, and the amount of L815A mutant seemed to be negligible compared with the wild type. These results may clarify the ambiguity of the microscopic observation of TLR4 (L815A) and TLR4 (L816A). Plasma membrane expression of TLR4 was impaired when the leucine at 815 or 816 was replaced to alanine. But the leucine at 815 is more critical, and the mutant L816A may show the weaker phenotypic change.

To further investigate the characteristics of the TLR4 (L815A) mutant, we performed an immunoprecipitation assay of wild-type and mutant TLR4. Cells were transfected with a human MD-2-FLAG-His_6 expression vector and either the wild-type or the mutant (L815A) TLR4-EGFP expression vector. Anti-TLR4 monoclonal antibody (clone HTA125), anti-GFP polyclonal antibody, or anti-FLAG monoclonal antibody was added to the lysate and precipitated with Protein G-Sepharose beads. Collected proteins were eluted and subjected to Western blotting. The results are shown in Fig. 8*C*. TLR4 (L815A) was not immunoprecipitated with anti-TLR4 antibody (HTA125). HTA125 antibody was raised against TLR4-expressing cells (9) and recognizes the extracellular portion of TLR4. This result suggests that the amino acid replacement at position 815 may cause a change in the extracellular portion of TLR4 and/or that the replacement may also inhibit cell surface expression of the mutant protein. On the other hand, both wild-type TLR4-EGFP and mutant TLR4-EGFP were immunoprecipitated with anti-GFP polyclonal antibody, which recognized EGFP. However, of the two bands of TLR4, the heavier band seems to be somewhat faint in the mutant, whereas in the wild type the heavier band is at least as dense as the lighter one. TLR4 can be detected as two separate bands in a Western blot (19), especially under transient transfection conditions. The difference in proportion of the heavy and light bands between wild-type and mutant TLR4 may suggest that there is some difference in glycosylation. Furthermore, wild-type TLR4 was coprecipitated with MD-2-FLAG-His_6, but the mutant TLR4 could not be detected (Fig. 8*C*, *lanes 4* and *8*). Because MD-2 is

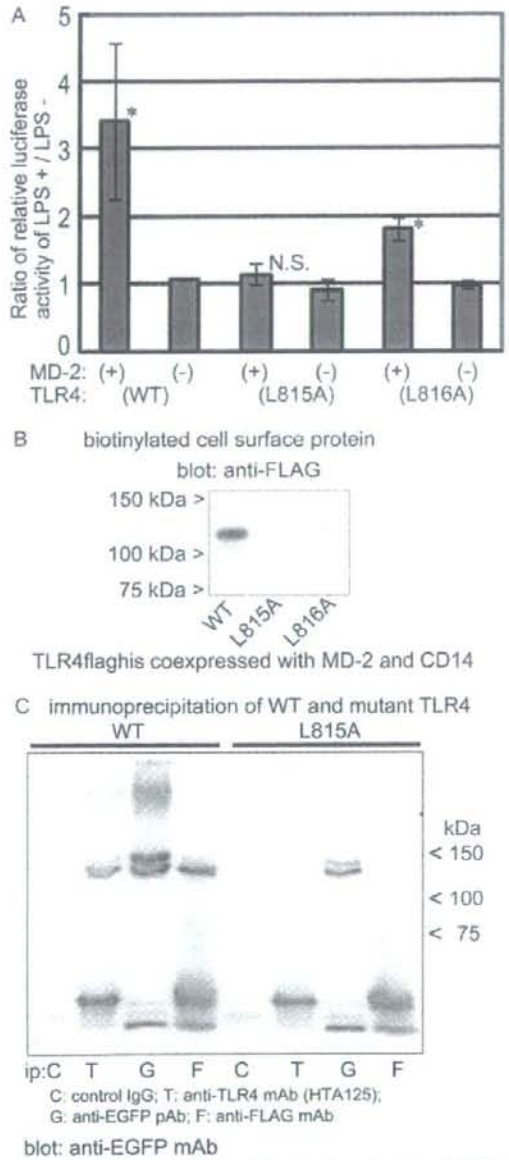

FIGURE 8. *A*, TLR4 mutants L815A and L816A with and without EGFP fusion exhibit the same phenotypes in LPS responsiveness and plasma membrane expression. HEK293T cells were transfected with the wild-type, the L815A or L816A mutant TLR4flaghis plasmid plus the human MD-2 plasmid and luciferase reporter, or control plasmids. After 36 h, cells were stimulated with LPS (10 ng/ml) for 7 h, and luciferase reporter gene activity was measured. The data were from three independent experiments. *Small bars* indicate 95% confidence intervals of the mean (*p* values for * are: TLR4 (WT) flaghis/MD-2 (+), $p = 0.046$; TLR4 (L816A) flaghis/MD-2 (+), $p = 0.003$). *N.S.*: not significant. *B*, wild-type and mutant TLR4s L815A and L816A were tagged by biotinylation of the cell surface proteins and affinity-purified. Human MD-2 and CD14 were coexpressed. TLR4 was visualized by immunoblotting using an anti-FLAG monoclonal antibody (*mAb*). Faint bands below 100 kDa are considered to be unbiotinylated intracellular TLR4 proteins that were not washed off during the process. Samples from TLR4 (WT), TLR4 (L815A), and TLR4 (L816A), respectively, were prepared from the same number of cells as for the biotinylation experiment. *C*, immunoprecipitation with antibodies further reveals the characteristics of TLR4 (L815A). Anti-TLR4 monoclonal antibody (HTA125) does not precipitate the mutant TLR4, whereas anti-GFP polyclonal antibody (*pAb*) precipitates both wild-type and mutant TLR4. Mutant TLR4 was not coprecipitated with MD-2-FLAG-His_6. Lysates were prepared from cells transiently expressing wild-type or mutant TLR4-EGFP and MD-2-FLAG-His_6.

associated with TLR4 (9), it is logical to expect that immunoprecipitating MD-2-FLAG-His_6 with anti-FLAG antibody should cause TLR4 to be coprecipitated with it. It is suggested by the result here that the association of the TLR4 mutant with MD-2 is impaired.

DISCUSSION

In this research, we performed mutagenesis analyses of particular amino acid residues in TLR4 to explore the mechanisms of TLR4 intracellular signal transduction and subcellular distribution. We found the candidate residues by analyzing truncation mutants of TLR4 in the cytoplasmic region, in which both signaling and normal subcellular distribution of TLR4 are disturbed. Because we are focusing on a common mechanism for the impaired signaling and distribution, we finally picked a single amino acid mutant that does not respond to LPS stimuli, as measured with NF-κB reporter luciferase assay, and one that does not localize on the plasma membrane. TLR4 (L815A) is a mutant that meets these conditions, and our results suggest that the leucine at position 815 of TLR4 is required for both signal transduction and plasma membrane localization.

The best known single amino acid mutant of TLR4 is TLR4 (P712H) known as the *Lps*^{d} mutation in the C3H/HeJ mouse, which corresponds to position 714 in this study of human TLR4 (5, 6, 20). Mice carrying this mutation opened up the rediscovery of TLR4 as a key player in innate immunity. Because this proline residue at this position is within the TIR domain and is conserved among TLRs or TLR4s of other species, it is assumed that the residue plays an important role in TLR4 function. The association of TLR4 (P712H) with its adapter proteins is reported to be intact, and the explanation for the functional impairment of TLR4 (P712H) is not clear (21–23).

Some single amino acid variants are found in humans, and these are related to the incidence or prognosis of some infections and other diseases. A growing body of data suggests that the ability of certain individuals to respond properly to TLR4 ligands may be impaired by single-nucleotide polymorphisms within TLR4 genes (24). The D299G and T399I alleles of the TLR4 gene have been associated with increased risk of severe infections (25).

By clarifying the subcellular component where the mutant protein is retained, or by clarifying to which compartment the mutant is not delivered, the abnormal intracellular sorting that is caused by the mutation in TLR4 (L815A) could be elucidated more precisely. Usually a sorting signal motif is comprised of several amino acids. In this regard, if the leucine at position 815 is a part of a motif, there should be other amino acids that are also members of the motif. Although replacement of leucine with alanine at position 816 did not cause an apparent signal transduction impediment, plasma membrane expression of TLR4 (L816A) was impaired to a certain extent. Positive

response to LPS stimulation by TLR4(L816A) could be attributable to this small amount of expression on the plasma membrane. Mutagenesis analyses of neighboring amino acids of the leucine at 815 were not definitive, but the results could be suggestive that the adjacent leucine at 816 may work together with the leucine at 815. Leucines at position 815 and 816 could be in the same motif, and the leucine at position 816 may be less critical.

Several proteins have been reported to be involved in TLR4 cell surface expression. Heat shock protein gp96 is necessary for TLR4 association with MD-2 in the ER and for subsequent cell surface expression (26). PRAT4A and PRAT4B are associated with TLR4 and regulate TLR4 cell surface expression (27, 28). In embryonic fibroblasts of MD-2 knockout mice, TLR4 localization on the cell surface is severely impaired, and most TLR4 is retained in the ER or Golgi apparatus (15). MD-2 binds to TLR4 at its extracellular domain and is essential for LPS recognition by TLR4 (29). Although proteins such as CD14 and LPS-binding protein are reported to have important roles in LPS recognition by TLR4, in an *in vitro* setting HEK293T cells gain LPS responsiveness by introducing only TLR4 and MD-2 genes when measured by NF-κB reporter assay (9, 30). Without transfection, HEK293 cells do not express TLR4, MD-2, or CD14, which are involved in LPS-induced intracellular signaling (31, 32). In this study, we show that the association of the TLR4 mutant and MD-2 is impaired (Fig. 8*C*).

Post-translational modification is another important factor for TLR4 function. Asparagine residues in the extracellular portion of TLR4 need to be glycosylated for plasma membrane expression of TLR4 (15, 19, 33). TLR4·MD-2 association is necessary for this glycosylation as well. The difference in the proportion of the heavy band to lighter band between wild-type and L815A mutant TLR4 immunoprecipitated with anti-GFP polyclonal antibody suggests that there may be some difference in glycosylation between wild-type and L815A mutant TLR4 (Fig. 8*C*). Although leucine at position 815 is located in the cytoplasmic tail of TLR4, we speculated that substitution of leucine at position 815 may cause a conformational change in the extracellular portion of the protein, which may interfere with the association between L815A mutant TLR4 and MD-2, leading to inhibition of glycosylation and cell surface expression of the mutant protein. Further investigation may reveal the mechanism involved in this phenotypic change in TLR4 (L815A), which would lead to better understanding of the mechanism of wild-type TLR4 signaling and trafficking.

Acknowledgment—We greatly appreciate the gift of human TLR4 and MD-2 cDNA from Dr. Kensuke Miyake (Institute of Medical Science, University of Tokyo, Japan).

REFERENCES

1. Takeda, K., Kaisho, T., and Akira, S. (2003) *Annu. Rev. Immunol.* **21,** 335–376
2. Hoebe, K., Du, X., Georgel, P., Janssen, E., Tabeta, K., Kim, S. O., Goode, J., Lin, P., Mann, N., Mudd, S., Crozat, K., Sovath, S., Han, J., and Beutler, B. (2003) *Nature* **424,** 743–748
3. Oshiumi, H., Sasai, M., Shida, K., Fujita, T., Matsumoto, M., and Seya, T. (2003) *J. Biol. Chem.* **278,** 49751–49762
4. Yamamoto, M., Sato, S., Mori, K., Hoshino, K., Takeuchi, O., Takeda, K., and Akira, S. (2002) *J. Immunol.* **169,** 6668–6672
5. Qureshi, S. T., Lariviere, L., Leveque, G., Clermont, S., Moore, K. J., Gros, P., and Malo, D. (1999) *J. Exp. Med.* **189,** 615–625
6. Poltorak, A., He, X., Smirnova, I., Liu, M. Y., Van Huffel, C., Du, X., Birdwell, D., Alejos, E., Silva, M., Galanos, C., Freudenberg, M., Ricciardi-Castagnoli, P., Layton, B., and Beutler, B. (1998) *Science* **282,** 2085–2088
7. Visintin, A., Mazzoni, A., Spitzer, J. A., and Segal, D. M. (2001) *Proc. Natl. Acad. Sci. U. S. A.* **98,** 12156–12161
8. Nishitani, C., Mitsuzawa, H., Hyakushima, N., Sano, H., Matsushima, N., and Kuroki, Y. (2005) *Biochem. Biophys. Res. Commun.* **328,** 586–590
9. Shimazu, R., Akashi, S., Ogata, H., Nagai, Y., Fukudome, K., Miyake, K., and Kimoto, M. (1999) *J. Exp. Med.* **189,** 1777–1782
10. Bonifacino, J. S., and Traub, L. M. (2003) *Annu. Rev. Biochem.* **72,** 395–447
11. Nishimura, N., and Balch, W. E. (1997) *Science* **277,** 556–558
12. Nufer, O., and Hauri, H. P. (2003) *Curr. Biol.* **13,** R391–393
13. Slack, J. L., Schooley, K., Bonnert, T. P., Mitcham, J. L., Qwarnstrom, E. E., Sims, J. E., and Dower, S. K. (2000) *J. Biol. Chem.* **275,** 4670–4678
14. Latz, E., Visintin, A., Lien, E., Fitzgerald, K. A., Monks, B. G., Kurt-Jones, E. A., Golenbock, D. T., and Espevik, T. (2002) *J. Biol. Chem.* **277,** 47834–47843
15. Nagai, Y., Akashi, S., Nagafuku, M., Ogata, M., Iwakura, Y., Akira, S., Kitamura, T., Kosugi, A., Kimoto, M., and Miyake, K. (2002) *Nat. Immunol.* **3,** 667–672
16. Hein, C., and Andre, B. (1997) *Mol. Microbiol.* **24,** 607–616
17. Beutler, B. (2000) *Curr. Opin. Immunol.* **12,** 20–26
18. Akashi, S., Ogata, H., Kirikae, F., Kirikae, T., Kawasaki, K., Nishijima, M., Shimazu, R., Nagai, Y., Fukudome, K., Kimoto, M., and Miyake, K. (2000) *Biochem. Biophys. Res. Commun.* **268,** 172–177
19. Ohnishi, T., Muroi, M., and Tanamoto, K. (2003) *Clin. Diagn. Lab. Immunol.* **10,** 405–410
20. Xu, Y., Tao, X., Shen, B., Horng, T., Medzhitov, R., Manley, J. L., and Tong, L. (2000) *Nature* **408,** 111–115
21. Dunne, A., Ejdeback, M., Ludidi, P. L., O'Neill, L. A., and Gay, N. J. (2003) *J. Biol. Chem.* **278,** 41443–41451
22. Fitzgerald, K. A., Palsson-McDermott, E. M., Bowie, A. G., Jefferies, C. A., Mansell, A. S., Brady, G., Brint, E., Dunne, A., Gray, P., Harte, M. T., McMurray, D., Smith, D. E., Sims, J. E., Bird, T. A., and O'Neill, L. A. (2001) *Nature* **413,** 78–83
23. Horng, T., Barton, G. M., and Medzhitov, R. (2001) *Nat. Immunol.* **2,** 835–841
24. Schroder, N. W., and Schumann, R. R. (2005) *Lancet Infect. Dis.* **5,** 156–164
25. Agnese, D. M., Calvano, J. E., Hahm, S. J., Coyle, S. M., Corbett, S. A., Calvano, S. E., and Lowry, S. F. (2002) *J. Infect. Dis.* **186,** 1522–1525
26. Randow, F., and Seed, B. (2001) *Nat. Cell Biol.* **3,** 891–896
27. Wakabayashi, Y., Kobayashi, M., Akashi-Takamura, S., Tanimura, N., Konno, K., Takahashi, K., Ishii, T., Mizutani, T., Iba, H., Kouro, T., Takaki, S., Takatsu, K., Oda, Y., Ishihama, Y., Saitoh, S., and Miyake, K. (2006) *J. Immunol.* **177,** 1772–1779
28. Konno, K., Wakabayashi, Y., Akashi-Takamura, S., Ishii, T., Kobayashi, M., Takahashi, K., Kusumoto, Y., Saitoh, S., Yoshizawa, Y., and Miyake, K. (2006) *Biochem. Biophys. Res. Commun.* **339,** 1076–1082
29. Nishitani, C., Mitsuzawa, H., Sano, H., Shimizu, T., Matsushima, N., and Kuroki, Y. (2006) *J. Biol. Chem.* **281,** 38322–38329
30. Akashi, S., Shimazu, R., Ogata, H., Nagai, Y., Takeda, K., Kimoto, M., and Miyake, K. (2000) *J. Immunol.* **164,** 3471–3475
31. Espevik, T., Latz, E., Lien, E., Monks, B., and Golenbock, D. T. (2003) *Scand. J. Infect. Dis.* **35,** 660–664
32. Muta, T., and Takeshige, K. (2001) *Eur. J. Biochem.* **268,** 4580–4589
33. da Silva Correia, J., and Ulevitch, R. J. (2002) *J. Biol. Chem.* **277,** 1845–1854

Jpn. J. Infect. Dis., 62, 20-25, 2009

Original Article

Evaluation of a New Rapid Molecular Diagnostic System for *Plasmodium falciparum* Combined with DNA Filter Paper, Loop-Mediated Isothermal Amplification, and Melting Curve Analysis

Mariko Yamamura*, Koichi Makimura[1], and Yasuo Ota

Department of Internal Medicine, Teikyo University School of Medicine, Tokyo 173-0003, and [1]Teikyo University Institute of Medical Mycology, Teikyo University, Tokyo 192-0395, Japan

(Received August 25, 2008. Accepted November 12, 2008)

SUMMARY: Falciparum malaria is a fatal infection without immediate diagnosability or treatment. There are shortages of clinicians and examiners skilled in the treatment of malaria in non-endemic countries, including Japan. This study was performed to evaluate a novel rapid molecular diagnostic system consisting of loop-mediated isothermal amplification (LAMP) combined with DNA filter paper (FTA card) and melting curve analysis. Combining LAMP with melting curve analysis enabled diagnosis of *Plasmodium falciparum* more accurately with relative ease. FTA cards could be used to clarify problems regarding storage, infectivity, and transportation. The LAMP assay was carried out at a constant temperature of 63°C for 90 min. The diagnostic system (malaria-LAMP) accurately diagnosed malaria (47 samples from Thailand and 50 from Zimbabwe) with 97.8% sensitivity and 85.7% specificity as compared with microscopic methods, indicating the usefulness of this combined system.

INTRODUCTION

Malaria is one of the most important tropical infectious diseases. From 350 to 500 million clinical episodes of malaria occur each year, and the disease is responsible for more than 1 million deaths annually (1). Especially, *Plasmodium falciparum* causes various complications and may be fatal. The range of areas inhabited by malaria-carrying mosquitoes is currently expanding due to global climate change (2). Therefore, there is a risk of a revival of malaria, not only as a consequence of the increasing number of imported cases with the increase in overseas travelers, but also as a result of the growth of habitats suitable for malaria-carrying mosquitoes. Thus, the rapid diagnosis of this disease is extremely important. Malaria has been diagnosed by microscopic examination using Giemsa stain. However, diagnosis by microscopic examination requires skill, and may be difficult in cases where preventative oral medication was taken before onset, as well as in cases where the level of malaria parasite infection is low (3). In countries where malaria is not endemic, there are shortages of physicians and microscopy-skilled laboratory staff specializing in malaria, and thus the diagnosis of malaria is difficult. In recent years, simple kits have been developed to detect malaria parasite-specific proteins and enzymes as auxiliary diagnostic procedures. However, these kits have a number of problems, such as false positives in patients with rheumatoid factor or in the elderly (4). In addition, these kits are not commercially available in Japan, and are not in common use. Methods for genetic diagnosis of malaria using PCR are also being developed, and there have been reports of cases in which various types of malaria parasites were identified and multiple infections were diagnosed by detecting malaria-specific DNA sequences. However, PCR-based methods require complex procedures, expensive inspections, and several hours before a diagnosis can be made. Therefore, it is necessary to develop a simple, stable, and rapid method for diagnosing malaria. Loop-mediated isothermal amplification (LAMP) (5) meets these requirement and has been put to practical use as a sensitive detection method for many infections (severe acute respiratory syndrome [SARS] coronavirus [6], West Nile virus [7], avian influenza virus [8], norovirus [9], and *Legionella* bacteria [10]). The LAMP method for *P. falciparum* malaria has already been reported by Poon et al. (11) and Han et al. (12) The LAMP method is simple to perform and is less influenced by inhibitors than polymerase chain reaction (PCR) is. To identify LAMP products, it is necessary to develop methods such as restriction enzyme digestion and the confirmation of specific DNA ladder formation by electrophoresis (12). However, to avoid contamination from dispersion of the amplification products during electrophoresis, there has been a demand for simpler and safer technology to identify amplification products. To safely distinguish specific amplification products from non-specific primer-dimers often seen in LAMP, melting temperature curve analysis was used. *P. falciparum* malaria-specific LAMP primers were designed and FTA cards (Whatman, Kent, UK) were used to allow storage, transportation, and extraction of template DNA safely, stably, and easily from blood samples at room temperature. In this study, a new rapid molecular diagnostic system for *P. falciparum* was developed by combining DNA filter paper (FTA cards), LAMP, and melting curve analysis.

The applicability of this system was examined using 97 specimens from Thailand and Zimbabwe where *P. falciparum* malaria is endemic.

MATERIALS AND METHODS

***P. falciparum* strain and DNA extraction**: **(i) *P. falciparum* strain**: The malaria parasite used for DNA extraction was a strain of *P. falciparum* (FCN-1/Nigeria [13])

*Corresponding author: Mailing address: Department of Internal Medicine, Teikyo University School of Medicine, 2-11-1 Kaga, Itabashi, Tokyo 173-0003, Japan. Tel & Fax: +81-3-3964-2194. E-mail: yamariko829@excite.co.jp

maintained at the Department of Microbiology, School of Medicine, Teikyo University, Tokyo, Japan.

(ii) DNA extraction: The DNA of *P. falciparum* was extracted as follows. The strain was cultured for 3 days in flat-bottomed 96-well microtiter plates. The total volume of medium (RPMI1640 with 10% human serum) in each well was 200 μl, each of which contained 10% erythrocytes and 1% infected blood cells. The supernatant fluid in each well was discarded, and the remaining erythrocytes (including *P. falciparum*) were harvested and frozen at −80°C. The contents were thawed to induce hemolysis, after which distilled water and an equal amount of 1.8% NaCl were added. The mixture was centrifuged at 2,500 rpm for 10 min and the supernatant was discarded. These steps were repeated several times until the supernatant changed from pink to colorless. After heating the remaining pellet at 100°C for 15 min, the DNA was extracted by phenol/chloroform extraction and ethanol precipitation, and used as a template for amplification.

(iii) Preparation of plasmid for sensitivity test: The target sequence for LAMP assay was amplified by PCR using a primer pair (MAL-1, 5'-ACAGATTAAGCCATGCAAGT GA-3'; and MAL-2, 5'-AAACTTCCTTGTGTTAGATACAC-3') designed according to the 18S rDNA gene of *P. falciparum* (DDDJ/EMBL/GenBank accession no. AL031746). The PCR products were cloned and transformed using an Original TA Cloning Kit® (Invitrogen, Carlsbad, Calif., USA) in accordance with the manufacturer's instructions. The cloning plasmids were extracted from the transformed *Escherichia coli* using an Aurum Plasmid Mini Kit® (Bio-Rad Laboratories, Hercules, Calif., USA) in accordance with the manufacturer's instructions. These plasmids, which were diluted from 10,000 to 5 copies/tube by doubling dilution, were used as control plasmids (c-plasmid) for the sensitivity test to determine the detection limit.

Clinical samples and DNA elution: (i) Clinical samples: Samples of suspected malaria from Thailand (n = 47) and Zimbabwe (n = 50) were prepared by local staff in each area, who took blood samples from patients and directly deposited a few drops of the sample onto FTA cards for molecular diagnosis. As negative controls, normal whole blood samples on FTA cards from 59 individuals with no history of malaria infection (20 healthy individuals and 39 febrile patients, including those with leukopenia) were used. The study protocol was approved by the corresponding Ethical Committees of Teikyo University School of Medicine. All patients gave their informed consent to participate in the study.

(ii) Preparation of blood smears and microscopic examination: For thin blood smears, a single drop of whole blood was placed on a glass slide, immediately spread using a coverglass, and put aside to dry. After methanol fixation, the smears were stained with Giemsa solution.

For thick blood smears, one or two drops of whole blood were placed on a glass slide. The blood was spread to about 1 cm in diameter and put aside to dry. After drying, these smears were stained with Giemsa solution.

Thin and thick blood smears were prepared from 47 patients with suspected malaria infection in Thailand; a microscopist in Thailand provided the results of microscopic examination. Only thick blood smears were prepared from 50 patients with suspected malaria infection in Zimbabwe, and the results of the microscopic examination were unknown. All 97 blood smears were examined for the presence of malaria parasites at the Department of Microbiology, School of Medicine, Teikyo University. To calculate the infection rate in a thin blood smear, the number of infected erythrocytes was counted in increments of 10,000 erythrocytes. To calculate the infection rate in a thick blood smear, the number of infected erythrocytes was counted in increments of several leukocytes, depending on the smear. The results of microscopic examination were compared with those of malaria-LAMP assay using FTA cards.

(iii) DNA extraction from FTA card samples, and transport of FTA card samples: FTA cards with whole blood deposits were dried and stored at room temperature, and were then mailed to Japan. Disks 2.0 mm in diameter were cut from the bloodstained areas with a Harris Micro Punch (2.0 mm; Whatman). Each disk was washed three times with 200 μl of FTA purification reagent and twice with 200 μl of TE-1 buffer (10 mM Tris-HCl, 0.1 mM EDTA, pH 8.0). The disks were dried and used directly as the DNA template.

Oligonucleotide primers for LAMP reaction: The 18S rRNA gene nucleotide sequences were obtained for eight *Plasmodium* spp., including four species of human malaria parasite (*P. falciparum*, accession no. AL031746, NC004325; *P. ovale*, AB182489, AB182493; *P. vivax*, U03079, AY579418; *P. malariae*, AF145336; *P. knowlesi*, AY327557) from DDDJ/EMBL/GenBank Database, and by using DNA analysis software (GENETYX®-Mac ver.13; GENETYX, Tokyo, Japan). Six sites of specific nucleotide sequences of *P. falciparum* were determined as the primer sets. One pair of primers (F3 and B3) was designed based on the sequences at two sites in the outermost region, while another pair of primers (FIP and BIP) was designed to connect the sequences at two sites in the inner region. Thus, four primers were prepared for LAMP assay to detect *P. falciparum* genes. In addition, one pair of loop primers corresponding to this malaria-LAMP system was also designed. The location and nucleotide sequence of each primer are shown in Table 1.

The results of BLAST (Basic Local Alignment Search Tool) (14) analysis against DDBJ/EMBL/GenBank databases indicated that the sequences of malaria-LAMP primers were specific only for *P. falciparum*. Species-specific LAMP primer sets for *P. falciparum* (11) and *P. vivax* (12) were also used. The specificity of malaria-LAMP primers was tested with each of four species of human malaria DNA. Template DNAs for three malaria parasites, *P. vivax*, *P. malariae*, and *P. ovale*, were provided by Dr. Tsuboi, Ehime University, Japan (12).

Malaria-LAMP condition and melting curve analysis: The LAMP reaction was performed with a Loopamp DNA amplification kit (Eiken Chemical Co., Ltd., Tokyo, Japan). The reaction mixtures (25 μl) contained 40 pmol of primers FIP and BIP, 40 pmol of primers loopF and loopB, and 10 pmol of primers F3 and B3, 2 × reaction mixture (12.5 μl), 1 μl *Bst* DNA polymerase, 0.5 μl of YO-PRO®-1 iodide (Molecular Probes, Eugene, Oreg., USA), 1 to 3 μl of DNA sample, and distilled water (made up to a final volume of 25 μl/tube). The LAMP reaction was performed at 63°C for 90 min. As negative controls, several tubes containing distilled water supplied with the kit were also prepared per the reaction. The c-plasmid was used as a positive control at 10^7 copies/reaction. LAMP products were identified by melting curve analysis. Melting temperature curves were obtained using the default settings recommended by the manufacturer in the presence of a fluorescent interchelator (YO-PRO®-1 iodide). Amplification and melting curve analysis were carried out using a Genopattern Analyzer GP1000 (Yamato Scientific Co., Ltd., Tokyo, Japan).

Table 1. Malaria-LAMP primers

A	F3	gaggtgaaattctaagattttct	
	FIP(F1c+F2)	cacctagtcggtatagtttatggtgcctaatctatttccattaat F1c F2	
	B3c	ttccgtcaattctttttaacttte	
	BIP(B1+B2c)	gtagcatttcttagggaatgttggccccagaacccaaagacttttga B1 B2c	
	Loop F	ggtatctgatcgtcttcactccc	
	Loop B	gaat tgcttccttc agtaccttta	
B	1001	tcaggaggtgaaattctaagattttctggagacggactactgcgaaagcat F3	1050
	1051	ttgcctaatctatttccattaatcaagaacgaaagttaagggagtgaaga FIP(F2) loop F	1100
	1101	cgatcagataccgtcgtaatcttaaccataaactataccgactaggtgtt FIP(F1)	1150
	1151	ggatgaatataaaaaatatatataatatgtagcatttcttagggaatgttg BIP(B1)	1200
	1201	attttatattagaattgcttccttcagtaccttatgagaaatcaaagtct loop B BIP(B2)	1250
	1251	ttgggttctgggggcgagtattcgcgcaagcgagaaagttaaaagaattga B3	1300
	1301	cggaagggcaccacc	1315

A: Sequences of malaria-LAMP primers FIP, BIP, F3, B3, LoopF, and LoopB are used in this study.

B: Locations and sequences of malaria-LAMP target sequence and primer binding sites of *P. falciparum*. The locations of the primer binding site in the reference sequence (18SrRNA, GenBank accession no. AL031746) are underlined. Base numbers in the reference sequence are indicated at both ends.

RESULTS

Sensitivity and specificity: The malaria-LAMP system was able to detect c-plasmid at 10 copies/tube, but not at 5 copies/tube (Fig. 1). All of the melting curve peaks ($10-10^4$ copies/tube) obtained in this sensitivity test with c-plasmid were consistent (Fig. 2). The time required to amplify 10^4 copies/tube was 35 min, and that to amplify 10 copies/tube, which was decided as the detection limit, was 60-80 min.

The malaria-LAMP system was specific only for *P. falciparum* genomic DNA and c-plasmid, not for the three other human pathogenic malaria parasites. The peaks of the melting temperature curves were identical in genomic DNA and c-plasmid products. However, no melting temperature curves were obtained from other species of malaria parasite, because no products were amplified from their template DNAs (Fig. 3).

Application of malaria-LAMP to clinical samples: (i) Results of microscopic examination: Thailand (Table 2): A local microscopist examined all 47 samples of clinically suspected malaria infection, and found that 29 samples indicated the presence of *P. falciparum* parasites, while 4 samples

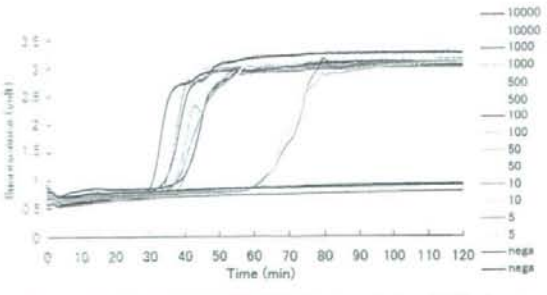

Fig. 1. Sensitivity of malaria-LAMP with control plasmid. The lower limit of detection of malaria-LAMP was 10 copies/tube, diluted from 10,000 to 5 copies/tube by doubling dilution.

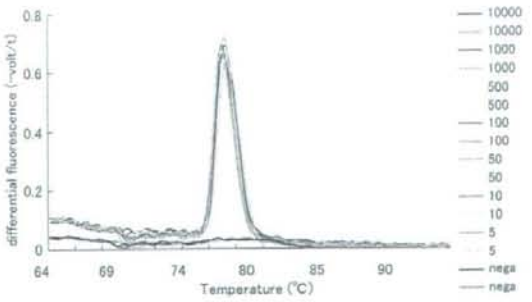

Fig. 2. Melting temperature curves of malaria-LAMP with control plasmid. The peaks of melting temperature curves of malaria-LAMP products amplified from control plasmid coincided with those from clinical specimens.

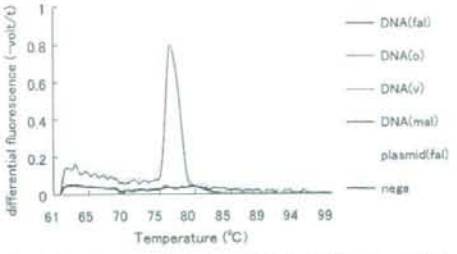

Fig. 3. Melting curve analysis for malaria-LAMP products. Malaria-LAMP amplified only *P. falciparum* genomic DNA and control plasmid, and their peaks of melting temperature curve were identical. DNA(fal), *P. falciparum* genomic DNA; DNA(o), *P. ovale* genomic DNA; DNA(v), *P. vivax* genomic DNA; DNA(mal), *P. malariae* genomic DNA.

Table 2. Comparison of results of malaria-LAMP and microscopy for 47 patients from Thailand

Patient no.	Diagnosis	Malaria-LAMP	Parasitemia of thin blood smears (%erythrocyte)	
			Microscopist (Teikyo University)	Microscopist (Thailand)
1	*P. falciparum*	+	6.12	13.4
2	*P. falciparum*	+	5.04	−
3	*P. falciparum*	+	4.98	1.8
4	*P. falciparum*	+	1.77	2.2
5	*P. falciparum*	+	1.71	0.9
6	*P. falciparum*	+	1.62	2
7	*P. falciparum*	+	1.5	1.5
8	*P. falciparum*	+	1.26	0.5
9	*P. falciparum*	+	0.87	−
10	*P. falciparum*	+	0.78	0.9
11	*P. falciparum*	+	0.74	0.7
12	*P. falciparum*	+	0.63	1
13	*P. falciparum*	+	0.63	1.1
14	*P. falciparum*	+	0.58	1.4
15	*P. falciparum*	+	0.51	0.3
16	*P. falciparum*	+	0.51	0.6
17	*P. falciparum*	+	0.39	0.3
18	*P. falciparum*	+	0.33	0.4
19	*P. falciparum*	+	0.32	0.5
20	*P. falciparum*	+	0.25	0.6
21	*P. falciparum*	−	0.21	0.6
22	*P. falciparum*	−	0.2	0.4
23	*P. falciparum*	−	0.16	0.2
24	*P. falciparum*	+	0.15	0.3
25	*P. falciparum*	−	0.12	0.4
26	*P. falciparum*	+	0.09	0.1
27	*P. falciparum*	+	0.08	0.1
28	*P. falciparum*	+	0.07	−
29	*P. falciparum*	+	0.06	1.3
30	*P. falciparum*	+	0.05	−
31	*P. falciparum*	+	0.04	−
32	*P. falciparum*	+	0.03	−
33	*P. falciparum*	+	0.02	−
34	*P. falciparum*	+	0.02	0.1
35	*P. falciparum*	+	0.02	−
36	*P. falciparum*	+	0.01	−
37	*P. falciparum*	+	0.01	−
38	*P. falciparum*	+	0.009	0.1
39	*P. falciparum*	+	0.007	0.1
40	*P. falciparum*	+	0.007	−
41	*P. falciparum*	+	−	−
42	*P. falciparum*	+	ND	−
43	*P. falciparum*	−	0.0000654	−
44	*P. vivax*	−	0.03	0.2
45	*P. vivax*	−	0.21	0.5
46	*P. vivax*	−	0.06	0.2
47	*P. vivax*	−	0.06	0.3

ND: Microscopist was not able to count because the condition of the specimen was poor.
−: Result of LAMP reaction was negative, or indicated absence of malaria parasites.
+: Result of LAMP reaction was positive.

Table 3. Comparison of results of malaria-LAMP and microscopy for 50 patients from Zimbabwe

Patient no.	Diagnosis	Malaria-LAMP	Parasitemia of thick blood smears (/leukocyte)
			Microscopist (Teikyo University)
48	*P. falciparum*	+	many
49	*P. falciparum*	+	many
50	*P. falciparum*	+	many
51	*P. falciparum*	+	many
52	*P. falciparum*	+	many
53	*P. falciparum*	+	many
54	*P. falciparum*	+	many
55	*P. falciparum*	+	74.8/leukocyte
56	*P. falciparum*	+	51.3/leukocyte
57	*P. falciparum*	+	40.3/leukocyte
58	*P. falciparum*	+	35.5/leukocyte
59	*P. falciparum*	+	32.5/leukocyte
60	*P. falciparum*	+	20.5/leukocyte
61	*P. falciparum*	+	18.3/leukocyte
62	*P. falciparum*	+	13/leukocyte
63	*P. falciparum*	+	11.2/leukocyte
64	*P. falciparum*	+	11/leukocyte
65	*P. falciparum*	+	10.5/leukocyte
66	*P. falciparum*	+	9.7/leukocyte
67	*P. falciparum*	+	9.7/leukocyte
68	*P. falciparum*	+	8.7/leukocyte
69	*P. falciparum*	−	8.3/leukocyte
70	*P. falciparum*	+	8/leukocyte
71	*P. falciparum*	+	6.7/leukocyte
72	*P. falciparum*	+	6.2/leukocyte
73	*P. falciparum*	+	6/leukocyte
74	*P. falciparum*	+	6/leukocyte
75	*P. falciparum*	+	6/leukocyte
76	*P. falciparum*	+	4.7/leukocyte
77	*P. falciparum*	+	3.7/leukocyte
78	*P. falciparum*	+	3.2/leukocyte
79	*P. falciparum*	+	2.9/leukocyte
80	*P. falciparum*	+	2.6/leukocyte
81	*P. falciparum*	−	2.4/leukocyte
82	*P. falciparum*	−	2.4/leukocyte
83	*P. falciparum*	−	2.4/leukocyte
84	*P. falciparum*	−	2.4/leukocyte
85	*P. falciparum*	−	2/leukocyte
86	*P. falciparum*	−	2/leukocyte
87	*P. falciparum*	−	1.7/leukocyte
88	*P. falciparum*	+	1.5/leukocyte
89	*P. falciparum*	+	1.2/leukocyte
90	*P. falciparum*	+	1/leukocyte
91	*P. falciparum*	+	0.9/leukocyte
92	*P. falciparum*	+	0.6/leukocyte
93	*P. falciparum*	+	0.14/leukocyte
94	*P. falciparum*	+	few
95	−	−	−
96	−	−	−
97	−	+	−

Many: Large number of infected erythrocyte.
Few: A few infected erythrocyte per field.
−: Result of LAMP reaction was negative, or indicated absence of malaria parasites.
+: Result of LAMP reaction was positive.

showed the presence of *P. vivax* parasites in both thick and thin blood smears. Twelve samples (#9, #28, #30-32, #35-37, #40-43) showed the presence of *P. falciparum* parasites only in thick blood smears (i.e., they were absent in thin blood smears). The local microscopist was not able to detect parasites in 2 samples (#2, #33), but a microscopist at Teikyo University detected *P. falciparum* parasites in both of these samples. The diagnoses of the malaria parasite species were the same between Thailand and Teikyo University, although the infection rate in thin blood smears differed between the microscopists.

Zimbabwe (Table 3): A microscopist at Teikyo University examined 50 samples of clinically suspected malaria infe tion, and found that 47 samples were positive for the pr ence of *P. falciparum* parasites in thick blood smears, wher 3 samples (#95-97) did not have any parasites.

Results of malaria-LAMP of clinical samples: Malar LAMP was performed using template DNA extracted fr FTA card specimens of thin and thick blood smear samp from which *P. falciparum* was detected (90 cases; 43 fr Thailand, 47 from Zimbabwe). *P. vivax* was detected in samp from 4 cases. Howerer, remaining 3 cases were negative

microscopic examination. Melting temperature curves were used to identify the amplification product. The samples were defined as negative if the peaks of the melting temperature curves did not reach 2.5 the height of the peaks of the positive control using c-plasmid. All 90 cases of falciparum malaria showed gene amplification, but the peaks of the melting temperature curves of 2 cases (#43, #69) differed from those of *P. falciparum*, and the sensitivity of malaria-LAMP was 97.8%. Case #43 showed a very low infection rate of 0.0000654% on the thin blood smear sample.

In addition, 1 (#47) of the 4 cases of vivax malaria showed gene amplification, but the peaks on the melting temperature curves differed from those of *P. falciparum*, and thus could be distinguished from falciparum malaria. *P. vivax* DNA was amplified from this sample with *P. vivax*-specific LAMP reaction (12). Of the 3 cases that were negative on microscopic examination, 1 case (#97) showed gene amplification, while the remaining 2 (#95, 96) did not. *P. falciparum* DNA was also amplified from #97 with another *P. falciparum*-specific LAMP reaction (11). Assuming that the 3 cases that were negative on microscopic examination as diseases other than falciparum malaria, the specificity compared to microscopic examination was 85.7%.

The results of the microscopic examinations, as well as those of malaria-LAMP for specimens from Thailand and Zimbabwe, are shown in Tables 2 and 3, respectively.

The time required to confirm the reaction in clinical specimens using FTA cards was 33 - 85 min (average, 49 min).

Nonspecific amplification and characteristics of melting temperature curves: When this reaction was performed for FTA cards from 59 non-malaria cases, amplification was confirmed in 7 cases and in the negative control in one reaction. However, none of the melting temperature curves matched that for *P. falciparum*, so they were classified as nonspecific reactions. These nonspecific amplifications had at least one of the following characteristics: (i) no reproducibility of amplification; (ii) no reproducibility of peak positions of the melting temperature curves.

DISCUSSION

A number of reports have indicated that PCR's minimal detection level of PCR is from 1 to 10 copies/reaction (15-18). Therefore, the sensitivity of the system presented here is equivalent to that of PCR. The levels of microscopic examination by skilled laboratory staff are 10 - 30 parasites/μl in thick blood smear samples under optimal conditions (15), and theoretically the present method is equivalent to or better than microscopic examination. When samples of 125 μl of blood, a feasible sample volume according to the manufacturer's literature, are applied to FTA cards, the expected erythrocyte number on the disc is 3.6×10^6, and the detectable infection rate of malaria is theoretically as low as 0.000278% when the detection limit in the present system is 10 copies. The sensitivity for the clinical sample compared to the microscopic examination was 97.8%. The LAMP method is superior to PCR-based methods in that the procedures involved are less complex. The LAMP method is also superior to the microscopic method, which is affected by the skill of the individual microscopist, in its reproducibility. The present method could detect parasites in cases where the infection was undetectable on microscopic examination in thin blood smears. The specificity of this system compared to microscopic examination was 85.7%, because only 1 sample (#97) was shown to be negative on microscopic examination but was positive in malaria-LAMP. However, sample #97 was positive in another *P. falciparum*-specific LAMP reaction reported by Poon et al. (11). Therefore, considering #97 to be from a falciparum malaria patient, the specificity of the present method would be 100%.

Turbidimetry to visual observation (11,12), with which the malaria-LAMP products are identified, is both simple and accurate, but identification is expected to be difficult in some clinical samples. In addition, as the present paper indicated, there is a possibility of nonspecific amplification even for the LAMP method, and therefore the amplification products should always be checked. Melting curve analysis can automatically differentiate between specific and nonspecific amplification using commercially available real-time PCR analyzers. As reported previously (19), the process of agarose gel electrophoresis tends to cause severe contamination by dispersion of LAMP products, so melting-curve analysis was used rather than electrophoresis to confirm specific malaria-LAMP products. Melting temperature curves have been used to identify PCR products in diagnosing malaria or in identifying the species of malaria parasite (15,16). Although the application of melting curve analysis for LAMP products has already been reported to identify pneumocystis (19), this is the first report to identify the LAMP products of malaria using melting curves.

The cells in a sample are destroyed after they are dropped onto the FTA cards (specially processed filter paper) with DNA fixation. The cards can therefore be stored at room temperature and mailed. Indeed, the cards were obtained by mail from two countries in the present study (Thailand and Zimbabwe). In hospitals with no examination apparatus or skill for identifying malaria, mailing the FTA card presents a useful diagnostic opportunity. Zhong et al. (20) reported the usefulness of the FTA card in detecting malaria parasite DNA by PCR. Mas et al. (21) reported that the DNA recovery rate in samples of FTA cards was better in the presence of ethylenediaminetetraacetic acid (EDTA), and tubes containing EDTA were used to collect blood samples. The DNA synthetic enzyme in the LAMP method is unaffected by the presence of hemoglobin or excessive salt concentration, etc., while Taq DNA polymerase used in PCR (22) is affected by these conditions. Poon et al. (11) reported that they were able to use heat-treated whole-blood specimens directly as a DNA template for LAMP assay. However, in a preliminary experiment, we could not obtain stable results through DNA extraction by heat treatment, unlike the case using FTA cards. If pretreatment of FTA cards can be performed in 30 min, it would take approximately 2 h from blood sampling to obtain the results. Due to its rapidity and ease of use, as well as the lack of a requirement for specialized skill, this system will be useful in countries where malaria is not endemic, such as Japan. Using this system in combination with microscopic examination, it will be possible to obtain a more accurate diagnosis of malaria in clinical practice.

ACKNOWLEDGMENTS

We wish to express our gratitude to Prof. Kiseko Kamei of the former Department of Microbiology and Immunology, Teikyo University School of Medicine (currently Teikyo Heisei University), Dr. Ryuichi Fujisaki and Associate Prof. Hajime Nishitani of Internal Medicine, Teikyo University School of Medicine, and Mr. Masato Ishihara of Yamato Science Co. Ltd. for their valuable support. In addition, we wish to thank Prof. Takafumi Tsuboi, Cell-Free Science and Technology Research Center and Venture Business Laboratory, Ehime University, for providing malaria DNA.

REFERENCES

1. World Health Organization (2003): The World Health Report 2003: Shaping the Future. World Health Organization, Geneva.
2. Patz, J.A. and Olson, S.H. (2006): Malaria risk and temperature: influences from global climate change and local land use practices. Proc. Natl. Acad. Sci. USA, 103, 5635-5636.
3. Haranaga, S., Akashi, M., Yara, S., et al. (2002): Two cases of mixed infection of malaria diagnosed by PCR method. J. Jpn. Assoc. Infect. Dis., 76, 571-575 (in Japanese).
4. Kano, S. (2006): Malaria rapid diagnostic kit. MEDICO, 37, 36-40 (in Japanese).
5. Notomi, T., Okayama, H., Masubuchi, H., et al. (2000): Loop-mediated isothermal amplification of DNA. Nucleic Acids Res., 28, E63.
6. Hong, T.C., Mai, Q.L., Cuong, D.V., et al. (2004): Development and evaluation of a novel loop-mediated isothermal amplification method for rapid detection of severe acute respiratory syndrome coronavirus. J. Clin. Microbiol., 42, 1956-1961.
7. Parida, M., Posadas, G., Inoue, S., et al. (2004): Real-time reverse transcription loop-mediated isothermal amplification for rapid detection of West Nile virus. J. Clin. Microbiol., 42, 257-263.
8. Imai, M., Ninomiya, A., Minekawa, H., et al. (2006): Development of H5-RT-LAMP (loop-mediated isothermal amplification) system for rapid diagnosis of H5 avian influenza virus infection. Vaccine, 24, 6679-6682.
9. Fukuda, S., Takao, S., Kuwayama, M., et al. (2006): Rapid detection of norovirus from fecal specimens by real-time reverse transcription-loop-mediated isothermal amplification assay. J. Clin. Microbiol., 44, 1376-1381.
10. Annaka, T., Yoshino, M., Momoda, T., et al. (2003): Rapid and simple detection of *Legionella* species by LAMP, a new DNA amplification method. J. Jpn. Soc. Clin. Microbiol., 13, 19-25 (in Japanese).
11. Poon, L.L., Wong, B.W., Ma, E.H., et al. (2006): Sensitive and inexpensive molecular test for falciparum malaria: detecting *Plasmodium falciparum* DNA directly from heat-treated blood by loop-mediated isothermal amplification. Clin. Chemother., 52, 303-306.
12. Han, E.T., Watanabe, R., Sattabongkot, J., et al. (2007): Detection of four *Plasmodium* species by genus- and species-specific loop-mediated isothermal amplification for clinical diagnosis. J. Clin. Microbiol., 45, 2521-2528.
13. Nguyen-Dinh, P. and Trager, W. (1980): *Plasmodium falciparum* in vitro: determination of chloroquine sensitivity of three new strains by a modified 48-hour test. Am. J. Trop. Med. Hyg., 29, 339-342.
14. Zhang, J. and Madden, T.L. (1997): PowerBLAST: a new network BLAST application for interactive or automated sequence analysis and annotation. Genome Res., 7, 649-656.
15. Swan, H., Sloan, L., Muyombwe, A., et al. (2005): Evaluation of a real-time polymerase chain reaction assay for the diagnosis of malaria in patients from Thailand. Am. J. Trop. Med. Hyg., 73, 850-854.
16. Mangold, K.A., Manson, R.U., Koay, E.S., et al. (2005): Real-time PCR for detection and identification of *Plasmodium* spp. J. Clin. Microbiol., 43, 2435-2440.
17. Wataya, Y. and Kimura, M. (1999): DNA diagnosis of malaria. J. Clin. Exp. Med., 191, 67-73 (in Japanese).
18. Kho, W.G., Chung, J.Y., Sim, E.J., et al. (2003): A multiplex polymerase chain reaction for a differential diagnosis of *Plasmodium falciparum* and *Plasmodium vivax*. Parasitol. Int., 52, 229-236.
19. Uemura, N., Makimura, K., Onozaki, M., et al. (2008): Development of a loop-mediated isothermal amplification method for diagnosing *Pneumocystis* pneumonia. J. Med. Microbiol., 57, 50-57.
20. Zhong, K.J., Salas, C.J., Shafer, R., et al. (2001): Comparison of IsoCode STIX and FTA gene guard collection matrices as whole-blood storage and processing devices for diagnosis of malaria by PCR. J. Clin. Microbiol., 39, 1195-1196.
21. Mas, S., Crescenti, A., Gasso, P., et al. (2007): DNA cards: determinants of DNA yield and quality in collecting genetic samples for pharmacogenetic studies. Basic Clin. Pharmacol. Toxicol., 101, 132-137.
22. Fujisaki, R. (2004): Development of rapid molecular diagnostic method for tuberculosis based on loop-mediated isothermal amplification. Teikyo Med. J., 27, 297-305 (in Japanese).

INTERNAL MEDICINE

□ CASE REPORT □

Combined Treatment with Oral Kanamycin and Parenteral Antibiotics for a Case of Persistent Bacteremia and Intestinal Carriage with *Campylobacter coli*

Haruka Okada[1], Takatoshi Kitazawa[1], Sohei Harada[1], Satoru Itoyama[1], Shuji Hatakeyama[1], Yasuo Ota[1,2] and Kazuhiko Koike[1]

Abstract

Campylobacter coli (*C. coli*) is a rare pathogen of bacteremia, but in immunocompromised hosts, *C. coli* occasionally causes bacteremia which can be refractory to antibiotic treatment. We report a case of *C. coli* bacteremia in a patient with X-linked agammaglobulinemia. Bacteremia relapsed repeatedly in spite of treatment with combined intravenous antibiotics. *C. coli* was observed in the biopsy specimens from the intestinal mucosa, suggesting intestinal carriage and reservoir of recurring infection. The addition of oral kamamycin with intravenous antibiotics was successful in eradicating *C. coli* from the blood and intestine.

Key words: *Campylobacter coli*, X-linked agammaglobulinemia, oral kamamycin

(Inter Med 47: 1363-1366, 2008)
(DOI: 10.2169/internalmedicine.47.1161)

Introduction

Campylobacter jejuni and *Campylobacter coli* (*C. coli*) frequently cause enteritis, but rarely cause bacteremia or extraintestinal infections in immunologically normal hosts (1, 2). However, in immunocompromised hosts, especially in patients with humoral immunodeficiency, these organisms occasionally develop prolonged, severe extraintestinal infection such as bacteremia, osteomyelitis, and arthritis (1, 3-5). We report a case of bacteremia, endocarditis, and osteomyelitis with *C. coli* in a patient with X-linked agammaglobulinemia. Bacteremia relapsed repeatedly in spite of treatment with combined intravenous antibiotics. *Campylobacter* was never isolated from stool cultures, but observed in the biopsy specimens from intestinal mucosa, suggesting the intestinal carriage. The addition of oral kamamycin with intravenous antibiotics was successful in eradicating *C. coli* from the blood, the bone and the intestine.

Case Report

A 33-year-old man with X-linked agammaglobulinemia was admitted to our hospital because of sustained fever and cellulitis of the left leg. The patient had history of recurrent diarrhea, upper respiratory infection and otitis media, and had been receiving immunoglobulin replacement therapy every two weeks. He had no history of overseas travel. He did not remember having raw meat such as chicken or coming into contact with animals in the past year. At the outpatient visits, oral cefcapene pivoxil and then intravenous ceftriaxone were administered, but the fever and cellulitis did not improve.

On admission, his temperature was 39.5℃, and his left leg was swollen. A grade 1/6 holosystolic cardiac murmur was heard. The abdomen was normal. The white blood cell count was 2,700/mm^3, the C reactive protein level was 1.09 mg/dL. The serum IgG was 893 mg/dL, but neither IgA nor IgM was detectable. Meropenem and then intravenous ciprofloxacin were administered for ten days. Seven days after discontinuation of the intravenous antibiotics, cel-

[1]Department of Infectious Diseases, Graduate School of Medicine, The University of Tokyo, Tokyo and [2]Department of Medicine, Teikyo University School of Medicine, Tokyo
Received for publication March 26, 2008; Accepted for publication April 25, 2008
Correspondence to Dr. Yasuo Ota, yasuota-tky@umin.ac.jp

Inter Med 47: 1363-1366, 2008 DOI: 10.2169/internalmedicine.47.1161

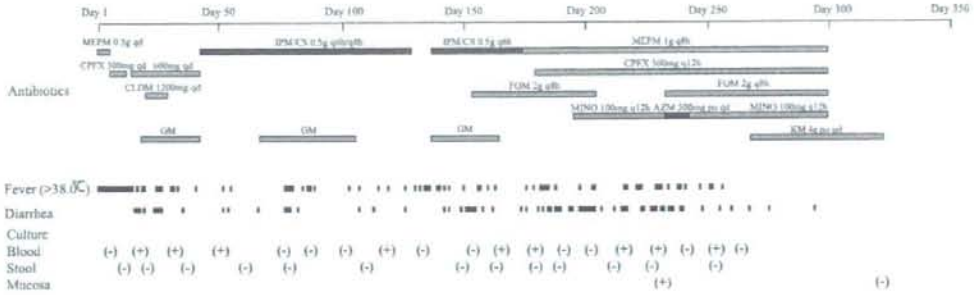

Figure 1. **Clinical course of the patient. Antibiotics are shown in the upper panel. Fever and diarrhea are shown in the middle panel. Cultures from blood, stool and the intestinal mucosa are shown in the lower panel. MEPM: meropenem, IPM/CS: imipenem/cilastatin sodium, CPFX: ciprofloxacin, CLDM: clindamycin, FOM: fosfomycin, MINO, minocycline, AZM: azithromycin, GM: gentamicin, KM: kanamycin.**

lulitis of his left leg worsened again. Blood culture was positive for *Campylobacter* species, which was determined as *C. coli* by a polymerase chain reaction assay. Stool cultures obtained repeatedly during the hospitalization did not yield *C. coli* (Fig. 1).

Intravenous administration of ciprofloxacin and gentamicin was started. Blood cultures continued to be positive for *C. coli*. A transesophageal echocardiography showed vegetation on the mitral valve, which suggested infective endocarditis. A colon fiberscope revealed mild inflammation. Antibiotics were switched to imipenem/cilastatin, and one week after the switch, blood culture turned negative. But four days after discontinuation of the 8-week antibiotic therapy, he became febrile again, and blood culture turned positive for *C. coli*. Intravenous imipenem/cilastatin and gentamicin were restarted. A magnetic resonance imaging study of the lower extremities revealed osteomyelitis of the left leg. Fosfomycin, which was susceptible in MIC test, was added to imipenem/cilastatin and gentamicin (Table 1). Gentamicin was discontinued because of renal tubular injury. Failing to eradicate *C. coli* from the blood, imipenem/cilastatin was switched to meropenem, ciprofloxacin and minocycline according to the susceptibility tests, and oral azithromycin, were sequentially added. In spite of disappearance of vegetation on the mitral valve in a transesophageal echocardiography and resolution of osteomyelitis of the left leg, bacteremia with *C. coli* continued (Fig. 1). During the combined antibiotic therapy, diarrhea and abdominal fullness became more prominent, although toxin A of *Clostridium difficile* was not detected from the stool. A colon fiberscope was performed again. The ascending colon was edematous, and the terminal ileum and the hepatic flexure were erosive. Although bacteria could not be detected histologically, all cultures of biopsy specimens sampled from the mucosa of the colon and the ileum yielded *Campylobacter* spp., suggesting intestinal carriage and reservoir of recurring infection.

Oral kanamycin was added to the intravenous antibiotics (Fig. 1). The following day his fever was resolved, and the abdominal symptoms improved. Blood cultures remained negative and intravenous antibiotics were discontinued six weeks after blood culture turned negative. A colon fiberscope was performed again, and oral kanamycin was discontinued after negativity of cultures of biopsy specimens from intestinal mucosa was confirmed. The total duration of oral kanamycin was ten weeks. The patient has been well for about eight months without relapse of bacteremia and diarrhea.

Table 1. **The Minimum Inhibitory Concentrations to Antimicrobial Agents against *Campylobacter Coli* Isolated from the Blood of Our Patient**

Antimicrobial agents	MIC (μg/mL)
Ampicillin	16.0
Sulbactam/ampicillin	32.0
Cefotaxime	>128.0
Cefpirome	>32.0
Aztreonam	>64.0
Imipenem/cilastatin	<0.5
Meropenem	<0.5
Gentamicin	<4.0
Erythromycin	8.0
Clarythromycin	8.0
Minocycline	16.0
Ciprofloxacin	8.0
Fosfomycin	<8.0

MIC: minimum inhibitory concentration

Discussion

Campylobacter coli is one of the most common *Campylobacter* species associated with diarrhea illness other than *C.*

Inter Med 47: 1363-1366, 2008 DOI: 10.2169/internalmedicine.47.1161

jejuni, and these two species produce clinically indistinguishable infections (6). *C. coli* are present not only in food animals such as poultry, cattle, sheep, pigs, but also in domestic pets. Since *Campylobacter* species other than *C. jejuni* are difficult to identify with phenotypic testing, tests for detection of species-specific sequences via PCR have been developed (7). Bacteremia caused by *Campylobacter* species is uncommon and usually resolves spontaneously in immunologically normal hosts (2). In compromised hosts however, prolonged, severe and recurrent *Campylobacter* bacteremia and other extraintestinal infections may occur (2-4). In such patients, intestinal tissue invasion of *Campylobacter* spp. may be one of the pathogenetic mechanisms (2, 5). In normal subjects with *C. jejuni/coli* enterocolitis, serum IgA, IgM, and IgG antibodies to *C. jejuni/coli* rise rapidly after infection, and IgA antibodies in intestinal secretions also increase (8, 9). In patients with hypogammaglobulinemia or infected with human immunodeficiency virus (HIV), an impaired antibody response to *C. jejuni/coli* infection including bacteremia has been noted (10, 11).

There have been eleven case reports of X-linked agammaglobulinemia with *Campylobacter* bacteremia (12-19). Among them six cases had stool cultures positive for *Campylobacter* species and the other five cases had no description about stool cultures. Furthermore, among the six positive stool culture cases, five cases had no gastrointestinal symptoms such as abdominal pain or diarrhea. We speculated that intestinal carriage of *Campylobacter* with or without gastrointestinal symptoms might be a risk factor of recurrent bacteremia in immunocompromised patients. Stool cultures had sensitivity of 40% for *Campylobacter* bacteremia (1). In the present patient, stool cultures were consistently negative for *C. coli*, but cultures of biopsy specimens from intestinal mucosa were positive for *C. coli*. Furthermore in our case, infective endocarditis and osteomyelitis were clinically resolved in spite of persistent bacteremia. We speculated that the intestinal tract would be a reservoir for *C. coli*. The mechanism of intestinal carriage of *Campylobacter* in immunocompromised patients remained unclarified, but it has been supposed that failure of humoral immune response in these patients might permit colonization of *Campylobacter* in the epithelium and lamina propria and induction of tissue damage (20, 21). A study on *Campylobacter* infections in 38 HIV-infected patients reported that in two patients with diarrhea, the cultures were positive only in the blood, and that in one patient a culture of biopsy specimen from intestinal mucosa yielded *C. jejuni* after disappearance in stool culture (22). We consider that in compromised patients, who are suspected to be infected with *Campylobacter* but have negative stool cultures for bacteria, culture of intestinal mucosa might be useful for diagnosing the intestinal carriage.

Macrolides and fluoroquinolones are antibiotic agents frequently used to treat *Campylobacter* infection (2). However, in *C. coli* bacteremia in compromised patients, treatment with these drugs might fail, and combined therapy of intravenous antibiotics such as carbapenems and aminoglycosides has been used (18). There have been three reports in which administration of oral antibiotics in addition to intravenous antibiotics were effective in eradicating *C. coli* from the intestine (12, 15, 18). In the present case, oral antibiotics other than azithromycin had not been tried until isolation of *C. coli* from the culture of intestinal mucosa, because the intestinal carriage had not been considered from mild nonspecific inflammatory findings in the first colonoscope and repeated negative stool culture. Intestinal biopsy was not performed in the previous reports, and this is the first case in which culture of intestinal mucosa was used for diagnosing the intestinal carriage with *C.coli* and confirming the eradication by the treatment with oral antibiotics. Oral kanamycin was selected in our case because the isolated *Campylobacter* strain was susceptible to gentamicin. Since aminoglycosides including kanamycin have poor bioavailability, we considered that oral administration of kanamycin could not reach a sufficiently high serum concentration to treat endocarditis or osteomyelitis, but the administration could reach a sufficient concentration in the intestinal mucosa for eradicating *Campylobacter* spp. from the intestine. We suggested that in a case of bacteremia and intestinal carriage with *Campylobacter* which was refractory to intravenous antibiotics, oral aminoglycoside therapy combined with intravenous antibiotics could be effective.

Acknowledgement

We would like to thank Mie Kataoka for preparing the manuscript.

References

1. Pigrau C, Bartolome R, Almirante B, Planes AM, Gavalda J, Pahissa A. Bacteremia due to *Campylobacter* species, clinical findings and antimicrobial susceptibility patterns. Clin Infect Dis **25**: 1414-1420, 1997.
2. Blaster MG, Bennett JE, Dolin R. *Campylobacter jejuni* and related species. In: Mandell, Douglas and Bennette's Principles and Practice of Infectious Diseases. 6th ed. Mandell GL, Douglas RG, Bennett JE, Eds. Elsevier/Churchill Livingstone, New York, 2005: 2276-2285.
3. Peterson MC. Clinical aspects of *Campylobacter jejuni* infections in adults. West J Med **161**: 148-152, 1994.
4. Akiba T, Akiba K, Suto N, Kumagai K, Sakamoto M, Yazaki N. *Campylobacter coli* bacteremia in an 11-year-old boy. Pediatr Int **44**: 543-544, 2002.
5. Ladron de, Guevara C, Gonzalez J, Pena P. Bacteraemia caused by *Campylobacter* spp. J Clin Pathol **47**: 174-175, 1994.
6. Fitzgerald C, Dolin R. *Campylobacter* and *Arcobacter*. In: Manual of Clinical Microbiology. 9th ed. Murray PR, Baron EJ, Jorgensen JH, et al, Eds. American Society for Microbiology, Washington, DC, 2007: 933-946.
7. Gonzalez I, Grant KA, Richardson PT, Park SF, Collins MD. Specific identification of the enteropathogens *Campylobacter jejuni*

Inter Med 47: 1363-1366, 2008 DOI: 10.2169/internalmedicine.47.1161

and *Campylobacter coli* by using a PCR test based on the ceuE gene encoding a putative virulence determinant. J Clin Microbiol **35**: 759-763, 1997.

8. Black RE, Perlman D, Clements ML. Human volunteer studies with *Campylobacter jejuni*. In: *Campylobacter jejuni*. Current Status and Future Trends. Nachmkin I, Blaser MJ, Topmpkins LS, Eds. American Society for Microbiology, Washington DC, 1992: 207-215.
9. Black RE, Levine MM, Clements ML, Hughes TP, Blaser MJ. Experimental *Campylobacter jejuni* infection in humans. J Infect Dis **157**: 472-479, 1988.
10. Johnson RJ, Nolan C, Wang SP, Shelton WR, Blaser MJ. Persistent *Campylobacter jejuni* infection in an immunocompromised patient. Ann Intern Med **100**: 832-834, 1984.
11. Perlman DM, Ampel NM, Schifman RB, et al. Persistent *Campylobacter jejuni* infections in patients infected with the human immunodeficiency virus (HIV). Ann Intern Med **1108**: 540-546, 1988.
12. Arai A, Kitano A, Sawabe E, Kanegane H, Miyawaki T, Miura O. Relapsing *Campylobacter coli* bacteremia with reactive arthritis in a patient with X-linked agammaglobulinemia. Intern Med **46**: 605-609, 2007.
13. van der Meer JW, Mouton RP, Daha MR, Schuurman RK. *Campylobacter jejuni* bacteraemia as a cause of recurrent fever in a patient with hypogammaglobulinaemia. J Infect **12**: 235-239, 1986.
14. Spelman DW, Davidson N, Buckmaster ND, Spicer WJ, Ryan P. *Campylobacter* bacteraemia: a report of 10 cases. Med J Aust **145**: 503-505, 1986.
15. Chusid MJ, Coleman CM, Dunne WM. Chronic asymptomatic *Campylobacter* bacteremia in a boy with X-linked hypogammaglobulinemia. Pediatr Infect Dis J **6**: 943-944, 1987.
16. Autenrieth IB, Schuster V, Ewald J, Harmsen D, Kreth HW. An unusual case of refractory *Campylobacter jejuni* infection in a patient with X-linked agammaglobulinemia: successful combined therapy with maternal plasma and ciprofloxacin. Clin Infect Dis **23**: 526-531, 1996.
17. Rafi A, Matz J. An unusual case of *Campylobacter jejuni* pericarditis in a patient with X-linked agammaglobulinemia. Ann Allergy Asthma Immunol **89**: 362-367, 2002.
18. Tokuda K, Nishi J, Miyanohara H, et al. Relapsing cellulitis associated with *Campylobacter coli* bacteremia in an agammaglobulinemic patient. Pediatr Infect Dis J **23**: 577-579, 2004.
19. Van der Hilst JC, Smits BW, van der Meer JW. Hypogammaglobulinaemia: cumulative experience in 49 patients in a tertiary care institution. Neth J Med **60**: 140-147, 2002.
20. Freeman AF, Holland SM. Persistent bacterial infections and primary immune disorders. Curr Opin Microbiol **10**: 70-75, 2007.
21. Wooldridge KG, Ketley JM. *Campylobacter*-host cell interactions. Trends Microbiol **5**: 96-102, 1997.
22. Molina J, Casin I, Hausfater P, et al. *Campylobacter* infections in HIV-infected patients: clinical and bacteriological features. Aids **9**: 881-885, 1995.

Antiviral Chemistry & Chemotherapy 19:133–141

Original article

Binding modes of two novel non-nucleoside reverse transcriptase inhibitors, YM-215389 and YM-228855, to HIV type-1 reverse transcriptase

Eiichi Kodama[1], Masaya Orita[2], Naoyuki Masuda[2], Osamu Yamamoto[2], Masahiro Fujii[2], Tetsuro Ohgami[2], Shunji Kageyama[2], Mitsuaki Ohta[2], Toshifumi Hatta[2], Hiroshi Inoue[2], Hiroshi Suzuki[2], Kenji Sudo[2], Yasuaki Shimizu[2] and Masao Matsuoka[1]*

[1]Laboratory of Virus Control, Institute for Virus Research, Kyoto University, Kyoto, Japan
[2]Drug Discovery Research, Astellas Pharma Inc., Tsukuba, Japan

*Corresponding author: E-mail: ekodama@virus.kyoto-u.ac.jp

Background: YM-215389 and YM-228855 are thiazolidenebenzenesulfonamide (TBS) derivatives and novel non-nucleoside reverse transcriptase inhibitors (NNRTIs) that inhibit not only wild-type, but also the K103N- and Y181C-substituted reverse transcriptase (RT) of HIV type-1 (HIV-1).

Methods: To characterize the binding modes of the TBS derivatives in detail, the anti-HIV-1 activities of YM-215389 and YM-228855 against various NNRTI-resistant clones were examined. Docking studies with HIV-1 RT were also performed.

Results: YM-215389, which effectively inhibits various NNRTI-resistant clones, interacted with L100, K103, V106 and Y318 through the benzene ring and with E138, V179, Y181, Y188 and W229 through the thiazole ring. A single amino acid substitution confers only moderate resistance to YM-215389; indeed, four amino acid substitutions (V106L, V108I, E138K and L214F) were necessary for high-level resistance. Although the activity of YM-228855, a derivative of YM-215389 that has two bulky and rigid cyano-moieties on the benzene ring, was 10× more potent against HIV-1 than YM-215389, its anti-HIV-1 activity was readily reduced with single substitutions as with Y181I and K103N.

Conclusions: These results provide structural information for optimizing the TBS derivatives in an attempt to construct ideal NNRTIs that maintain anti-HIV-1 activity to various HIV-1 variants.

Introduction

Allosteric inhibitors bind to a specific site on a target protein that differs from the substrate binding site and alters the conformation of the protein, resulting in a loss of protein function. Allosteric inhibitors for HIV type-1 (HIV-1) reverse transcriptase (RT), designated as non-nucleoside RT inhibitors (NNRTIs), are widely used for HIV-1-infected patients. NNRTIs bind to the NNRTI-binding hydrophobic pockets (NNRTI-BHP) located close to the RT active site and cause a conformational distortion to inactivate the enzyme [1].

Of the clinically approved NNRTIs, nevirapine (NVP) is used for pregnant women infected with HIV-1 to reduce the incidence of peripartum infection without severe adverse effects [2]. NVP combined with zidovudine (3′-azido-3′-deoxythymidine [AZT]) also effectively suppresses mother-to-child transmission during labour [3]. Efavirenz (EFV), another approved NNRTI, potently inhibits HIV-1 replication *in vitro* and in clinical cases [4]. In a clinical study, EFV administered with two nucleos(t)ide RT inhibitors (NRTIs) is more effective than a protease inhibitor administered with two NRTIs [5]. Moreover, during the initial treatment of HIV-1 infection, regimens that include EFV experience fewer treatment failures compared with regimens that include the NRTIs only [6–8]. Thus, the NNRTIs play an important role in the chemotherapy for HIV-1-infected patients.

Although NNRTIs potently inhibit HIV-1 replication, HIV-1 rapidly acquires resistance to NNRTIs, both *in vitro* and *in vivo*, through a conformational change in the NNRTI-BHP that is caused by mutations. NVP loses its anti-HIV-1 activity against HIV-1 variants that have amino acid substitutions, for example, lysine to aspartic acid at amino acid position 103 in the RT (K103N) or

Y181C variant [9–11]. The K103N variant and NNRTI-related double mutation, for example, K103N plus Y188L, carry high resistance to EFV [12,13]. Therefore, the development of NNRTIs, which maintain anti-HIV-1 activity against various NNRTI-resistant variants, is important to sustain long-term HIV-1 chemotherapy.

We recently reported that novel NNRTIs, the thiazolidenebenzenesulfonamide (TBS) derivatives YM-215389 and YM-228855 (Figure 1A), inhibited HIV-1 replication, including that of the K103N- and Y181C-substituted variants [14–16]. To elucidate YM-215389 and YM-228855 binding to HIV-1 RT, the anti-HIV-1 activity of these two TBS derivatives against NNRTI-resistant clones was measured. In addition, genotypic and phenotypic analyses of variants resistant to YM-215389 and YM-228855, as well as docking studies on these TBS derivatives with HIV-1 RT were performed. Our data provide useful structural information to optimize TBS derivatives for the ideal NNRTIs that maintain anti-HIV-1 activity to various HIV-1 variants.

Methods

Antiviral agents

AZT was purchased from Sigma (St Louis, MO, USA). NNRTIs, NVP, EFV, YM-215389 and YM-228855 were synthesized as described previously [14,17].

Cells

MT-2 and 293T cells were grown in RPMI 1640 medium and Dulbecco's modified Eagle's medium, respectively, supplemented with 10% fetal calf serum, 2 mM L-glutamine, 100 U/ml penicillin and 50 µg/ml streptomycin. HeLa-CD4-LTR/β-gal cells [18] were used to determine drug susceptibility.

Viruses and construction of HIV-1 clones

The laboratory strain, HIV-1_{LAI}, propagated in MT-2 cells, was employed for induction of the resistant variants. Recombinant infectious HIV-1 clones carrying various substitutions in the RT gene were generated as described previously [19]. Briefly, desired mutations were introduced into the *Xma*I–*Nhe*I region (759 base pairs) of pTZNX1, which codes for Gly-15 to Ala-267 of HIV-1 RT (strain BH10), by site-directed mutagenesis. The *Xma*I–*Nhe*I fragment was inserted into a pNL101-based plasmid, pNL–RT, generating various molecular clones with the desired mutations. The presence of the intended substitutions and the absence of unintended substitutions in the infectious clones were confirmed by sequencing.

Each molecular clone was transfected into 293T cells and cocultured with MT-2 cells after 24 h. When an extensive cytopathic effect was observed, cell-free supernatants were harvested, titrated for virus and stored at -80°C until use. An infectious clone generated from pNL–RT served as a wild-type infectious clone (HIV-1_{WT}).

Determination of drug susceptibility

The sensitivity of infectious clones to various RT inhibitors was determined using the multinuclear activation of a galactosidase indicator (MAGI) assay [18] with some modifications [19,20]. Briefly, HeLa CD4-LTR/β-gal cells (10^4 cells/well) were plated in 96-well flat microtitre culture plates. On the following day, the medium was aspirated and the cells were inoculated with the HIV-1 clones (70 MAGI units/well, which yielded 70 blue cells after 48 h of incubation) and cultured in the presence of various concentrations of drugs in fresh medium. The blue cells in each well were counted 48 h after viral exposure. All experiments were performed in triplicate.

Induction of resistant variants

MT-2 cells and HIV-1_{LAI} were used for induction of resistant variants using a dose-escalating method [20,21]. Each selection experiment began at the 50% effective concentration (EC_{50}) determined by the MAGI assay. When extensive cytopathic effects were observed, the concentration was increased to twice the initial concentration. The sequence of the RT region was determined using direct sequencing of the proviral DNA from the infected MT-2 cells.

Molecular modelling and docking studies

Three dimensional structures of YM-215389 and YM-228855 were generated using the previously determined crystal structure of the parental compound, *N*-(5-tert-butyl-3,4-dimethyl-1,3-thiazol-2(3*H*)-ylidene)-3-nitrobenzenesulfonamide [14,17] as the template. Docking studies of the compounds and HIV-1 RT were performed using the GOLD program [22] on the HIV-1 RT structure obtained from the Protein Data Bank (PDB) [23] for the 1HNV entry [24]. Structures of reference compounds, NVP and EFV (PDB code 1FK9 and 1VRT [25], respectively), were also obtained from the PDB. In these models, the amino acid substitution docking score for RT and the reference compounds were calculated using the SYBYL program, version 6.8 (Tripos, St Louis, MO, USA). To estimate the flexibility of YM-215389, we analysed the torsion angle distributions of the single rotation bond between the thiazole ring and the benzene ring using the Cambridge Structural Database (CSD) [26].

Results

Anti-HIV-1 activity of the TBS derivatives to NNRTI-resistant clones

The anti-HIV-1 activities of YM-215389 and YM-228855 against recombinant viruses with major NNRTI-resistant

substitutions (deposited in the Stanford HIV Drug Resistance Database [27,28]), were measured using the MAGI assay (Table 1). YM-215389 and YM-228855 inhibited six major substituted variants: HIV-1_{A98G}, HIV-1_{K103N}, HIV-1_{V106A}, HIV-1_{Y181C}, HIV-1_{V189I} and HIV-1_{G190A} with EC_{50} values at submicromolar concentrations. YM-215389 potently inhibited HIV-1_{V106A}, HIV-1_{Y181C} and HIV-1_{V189I} clones with EC_{50} values similar to that against HIV-1_{WT} (20 nM), but its anti-HIV-1 activity against HIV-1_{A98G}, HIV-1_{K103N} and HIV-1_{G190A} clones were somewhat less (7–33-fold resistance of HIV-1_{WT}). YM-228855, a derivative of YM-215389 that has two cyano-moieties on the phenyl ring, showed extremely potent anti-HIV-1 activity against HIV-1_{WT} (EC_{50}=2.0 nM). The anti-HIV-1 activity of YM-228855 against HIV-1_{A98G}, HIV-1_{K103N} and HIV-1_{Y181C} clones were less than against HIV-1_{WT} (17-, 87- and 54-fold, respectively). Interestingly, the anti-HIV-1 activity of YM-228855 against HIV-1_{V106A} and HIV-1_{V189I} was slightly more than against HIV-1_{WT}. Overall, the YM-215389 range of antiviral efficacy against NNRTI-resistant variants was larger than NVP and similar to EFV. However, the YM-228855 range of antiviral efficacy was similar to NVP, but worse than EFV and YM-215389 (Table 1).

Isolation and genotypic analyses of variants resistant to TBS derivatives

During serial passage (P) in the presence of YM-215389, at concentrations of <0.1 µM, a partial substitution of isoleucine for valine (V106V/I) and L214F substitutions were found at P-11 (Figure 1B). At P-16, V106V/I changed to solely V106I and additional partial substitutions, V108V/I and E138E/K, were identified. At P-20, at a concentration of >20 µM, the substitution of V106I changed to V106L and the partial substitutions V108V/I and E138E/K were completely changed to V108I and E138K, which resulted in a V106L, V108I, E138K and L214F combined mutant, HIV-$1_{YM\text{-}215389}{}^{R}$.

In the presence of YM-228855, at concentrations of <0.1 µM, T165I and L214F substitutions were found at P-16 (Figure 1C). These substitutions have not been reported as NNRTI-resistant substitutions, but are described as polymorphisms in the HIV-1 genome [29,30]. At P-24, partial substitutions for wild-type amino acids, V179V/D and Y188Y/C, were found in addition to the T165I and L214F mutations. However, at P-28, V179D disappeared and Y181Y/I emerged. At P-31, at concentrations >50 µM, T165I and Y188Y/C disappeared and the only detectable substitutions were

Table 1. Anti-HIV-1 activity of NNRTIs against various substituted variants

Virus	EC_{50}, nM (fold of resistance)				
	Zidovudine	Nevirapine	Efavirenz	YM-215389	YM-228855
HIV-$1_{NL\text{-}WT}$	32	40	0.5	20	2
Major NNRTI-resistant substitutions					
HIV-1_{A98G}	43 (1.3)*	192 (4.5)	2.7 (5.4)	184 (9.2)	34 (17)†
HIV-1_{K103N}	35 (1.1)	2,212 (55)†	47 (94)†	665 (33)†	199 (87)†
HIV-1_{V106A}	36 (1.1)	2,723 (68)†	2 (4)	22 (1.1)	0.4 (0.2)
HIV-1_{Y181C}	35 (1.1)	6,470 (160)†	0.7 (1.4)	46 (2.3)	107 (54)†
HIV-1_{V189I}	19 (0.6)	30 (0.8)	0.4 (0.8)	46 (2.3)	0.8 (0.4)
HIV-1_{G190A}	30 (1)	2,600 (65)*	4.5 (9)	145 (7.3)	12 (6)
Substitutions observed during selection with YM-215389					
HIV-1_{V106I}	18 (0.6)	94 (2)	0.7 (1.4)	52 (2.6)	3 (1.5)
HIV-1_{V106L}	21 (0.7)	33 (1)	0.5 (1)	310 (16)†	29 (15)†
HIV-1_{V108I}	1.9 (0.06)	473 (12)†	4.8 (10)†	66 (3.3)	4.8 (2.4)
HIV-1_{E138K}	2.8 (0.09)	156 (4)	2.5 (5)	174 (8.7)	10 (5)
HIV-1_{L214F}	6 (0.2)	69 (1.7)	1 (2)	35 (1.8)	3 (1.5)
HIV-$1_{V106I/E138K}$	10 (0.3)	430 (11)†	4 (8)	1,130 (57)†	43 (22)†
HIV-$1_{V106I/V108I/E138K}$	38 (1.2)	354 (9)	4 (8)	4,051 (200)†	44 (22)†
HIV-$1_{V106L/V108I/E138K}$	7 (0.2)	98 (2.5)	4 (8)	6,600 (330)†	106 (53)†
HIV-$1_{V106L/V108I/E138K/L214F}$	9 (0.3)	165 (4.1)	6 (12)†	>10,000 (>500)†	811 (400)†
Substitutions observed during selection with YM-228855					
HIV-1_{Y188C}	120 (4)	552 (14)	0.6 (1.2)	161 (8)	48 (24)
HIV-1_{Y181I}	30 (0.9)	7,150 (180)†	4.1 (8)	310 (16)†	1,084 (540)†
HIV-$1_{Y181I/L214F}$	25 (0.8)	>10,000 (>250)†	4 (8)	737 (37)†	2,874 (1,400)†

Data represent the mean values of at least three independent assays. The 50% antiviral effective concentration (EC_{50}) was determined from the multinuclear activation of a galactosidase indicator assay. *Fold of resistance compared with the HIV type-1 wild-type infectious clone (HIV-$1_{NL\text{-}WT}$). †Resistance >10-fold. NNRTI, non-nucleoside reverse transcriptase inhibitor.

Figure 1. Chemical structures of YM-215389 and YM-228855 and induction profiles of resistant variants

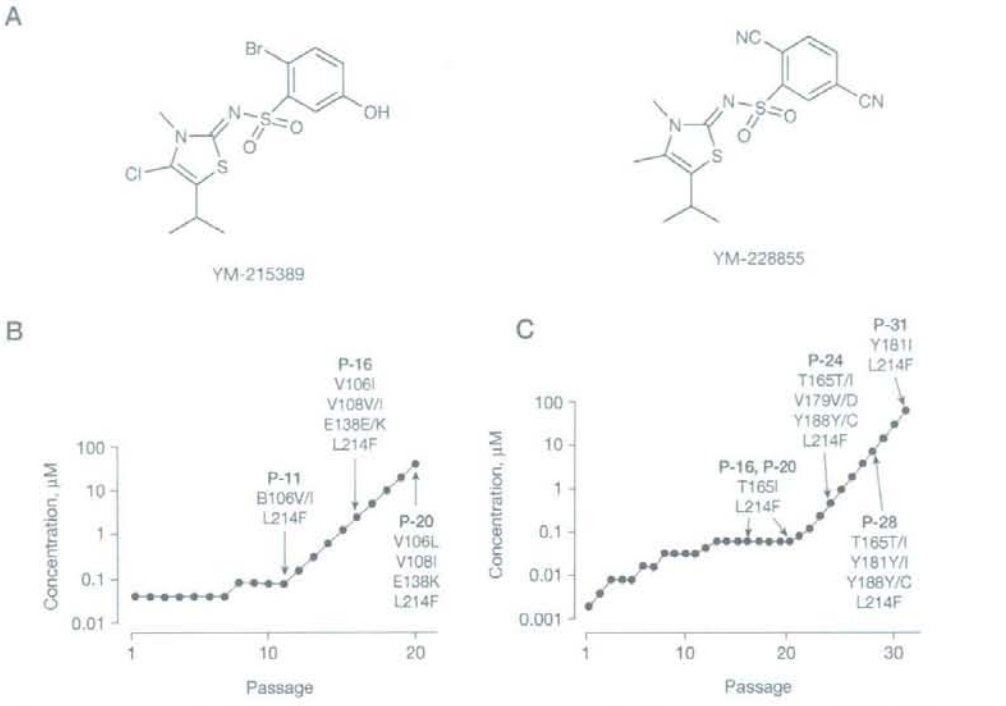

(A) Chemical structures of YM-215389 and YM-228855. The induction of resistant variants was performed using the dose-escalation method. (B) The HIV type-1 laboratory strain (HIV-1_{LAI}) was passed in the presence of increasing concentrations of YM-215389 and (C) YM-228855 in MT-2 cells. At the indicated passage (P), proviral DNA was extracted from HIV-1_{LAI}-infected MT-2 cells and subjected to PCR-mediated direct sequence analysis. The amino acid substitutions observed are shown. Each passage period was approximately 5–7 days.

Y181I and L214F (HIV-$1_{YM\text{-}228855}{}^{R}$). These changes might have some benefit for virus replication and/or the development of strong drug resistance. Although the resistant variants were selected in the presence of YM-215389 and YM-228855, which are structurally similar, their genotypes differ.

NNRTI-susceptibility of HIV-$1_{YM\text{-}215389}{}^{R}$ and HIV-$1_{YM\text{-}228855}{}^{R}$

YM-215389 and YM-228855 inhibited parental HIV-1_{LAI} replication (EC_{50} at 13 nM and 2.3 nM, respectively; Table 2). As expected, the variant resistant to YM-215389 (HIV-$1_{YM\text{-}215389}{}^{R}$) strongly reduced susceptibility to YM-215389 (>770-fold), but it showed only 140- and 17-fold reductions in susceptibility to YM-228855 and NVP, respectively. In contrast, the variant resistant to YM-228855 (HIV-$1_{YM\text{-}228855}{}^{R}$) exhibited high levels of resistance to YM-228855 (2,600-fold) and NVP (>250-fold), whereas it showed only 70-fold resistance to YM-215389. HIV-$1_{YM\text{-}215389}{}^{R}$ and HIV-$1_{YM\text{-}228855}{}^{R}$ showed a certain amount of cross-resistance to each other. Both variants showed a slight reduction in susceptibility to EFV (7–11-fold reduction). However, they showed different resistance phenotypes to NVP; HIV-$1_{YM\text{-}228855}{}^{R}$ reduced its susceptibility to NVP >15-fold stronger than HIV-$1_{YM\text{-}215389}{}^{R}$.

Effect of substitutions observed during the selection

To examine which substitution is involved in the development of YM-215389 and YM-228855 resistance, various molecular clones containing substitutions observed during the resistant variant selection were constructed. Among the substitutions obtained during HIV-$1_{YM\text{-}215389}{}^{R}$ selection, V106I, V106L and L214F substitutions did not confer any resistance to NVP or EFV (Table 1). The V106I substitution did not confer any resistance to TBS derivatives, whereas the V106L substitution resulted in modest resistance to YM-215389 and YM-228855 (16- and 15-fold reductions, respectively). The V108I substitution did not induce high resistance to TBS derivatives; however, it enhanced

Table 2. EC_{50} of NNRTIs for HIV-$1_{YM-215389}$* and HIV-$1_{YM-228855}$*

Virus	EC_{50} nM (fold of resistance)				
	Zidovudine	Nevirapine	Efavirenz	YM-215389	YM-228855
HIV-1_{WT}	21	40	0.7	13	2.3
HIV-$1_{YM-215389}$*	6 (0.29)*	680 (17)	8 (11)	>10,000 (>770)	325 (140)
HIV-$1_{YM-228855}$*	53 (2.5)	>10,000 (>250)	4.9 (7)	902 (69)	6,000 (2,600)

Data represent the mean values of at least three independent assays. The 50% antiviral effective concentration (EC_{50}) was determined from the multinuclear activation of a galactosidase indicator assay. *Fold of resistance compared with the HIV type-1 wild-type infectious clone (HIV-1_{NL4-3}). NNRTI, non-nucleoside reverse transcriptase inhibitor.

YM-215389 and YM-228855 resistance by E138K substitution. V108I and E138K substitutions are also observed during *in vitro* experiments with combination regimens containing EFV [31,32]. Comparisons of V106I/V108I/E138K with V106L/V108I/E138K also indicated that V106L enhanced drug resistance to TBS derivatives. This is consistent with observations made during selection; the V106I substitution was observed at P-16 (2.56 μM), but was replaced by V106L at P-20 (40 μM; Figure 1B). According to the Stanford HIV Drug Resistance Database, V106I is a common polymorphism that does not decrease NNRTI susceptibility. In contrast, V016L is rarely observed and only confers potential low-level resistance to NVP and delavirdine. Therefore, V106L appears to be a characteristic mutation for YM-215389.

The L214F substitution observed in many HIV-1 strains isolated from drug-naive patients [29] did not show resistance to any of the compounds tested. However, L214F enhanced resistance to YM-215389 when combined with V106L/V108I/E138K (Table 1). These results suggest that for the development of YM-215389 resistance, the primary mutation is V106L; however, other mutations are also needed to obtain stronger resistance (Table 1). L214F also played an important role in enhancing resistance to YM-228855 (Y181I with Y181I/L214F; Table 1).

Docking study

The modes in which YM-215389 and YM-228855 bind to HIV-1 RT were estimated using the GOLD program. Our simulation indicated that their binding modes are almost the same. As shown in Figures 2A–2D, 'the body' is formed by the hydrophilic sulfonamide faces outside of the NNRTI-BHP and 'the wings' are formed by the hydrophobic thiazole and benzene rings where they interact with the hydrophobic amino acids in the NNRTI-BHP, such as L100, K103, V106, Y318, E138, V179, Y181, Y188 and W229. YM-215389 interacts with L100, K103, V106 and Y318 through the benzene ring and with E138, V179, Y181, Y188 and W229 through the thiazole ring (Figure 2E). In our model, there was no hydrogen bonding between YM-215389 or YM-228855 and NNRTI-BHP. The T165 and L214 substitutions were located outside of the NNRTI-BHP and each had a slight effect on the binding of TBS derivatives to HIV-1 RT.

Structural comparison of TBS derivatives with NVP and EFV

The structures of YM-215389 and YM-228855 elucidated by our docking simulations were compared with those of NVP (1FK9) and EFV (1VRT). The TBS derivatives had a 'butterfly structure', like NVP and EFV (Figures 3A & 3B) [33,34]. The thiazole and benzene rings, and the sulfonamide region constitute the butterfly's left wing, right wing and body, respectively. Superimposition of the TBS derivatives' figures onto those of NVP and EFV shows that the wing and body sizes are similar to identical (Figure 3A). This indicates that TBS derivatives interact with the NNRTI-BHP in a manner similar to that of NVP and EFV.

Flexibility of TBS

In the CSD, 24 compounds with a thiazole ring-sulfonamide-benzene ring are deposited and were subjected to analysis of their torsion angles at C1-N2-S3-C4. The torsion angles were distributed between -123° to -64° and 71° to 129°. Conformational preferences for YM-215389 are depicted in Figure 4. Because the benzene ring must be in the upright position (as depicted in Figure 2) in order to interact with NNRTI-BHP, the torsion angle distribution of the wing-angle was estimated to be 71 to 129°, which suggests that the sulfonamide bond can be rotated intermediately.

Discussion

Currently available NNRTIs interact with the NNRTI-BHP close to the HIV-1 RT active site [35,36]. This common binding pocket results in cross-resistance among both first- and second-generation NNRTIs. For example, the K103N mutation located at the entrance to the NNRTI-BHP [37,38] reduces susceptibility to various NNRTIs. The transformation of the linearly charged amino acid lysine into uncharged and branched asparagine increases pocket volume and decreases interaction

Figure 2. Binding modes of YM-215389 and YM-228855 to NNRTI-BHP

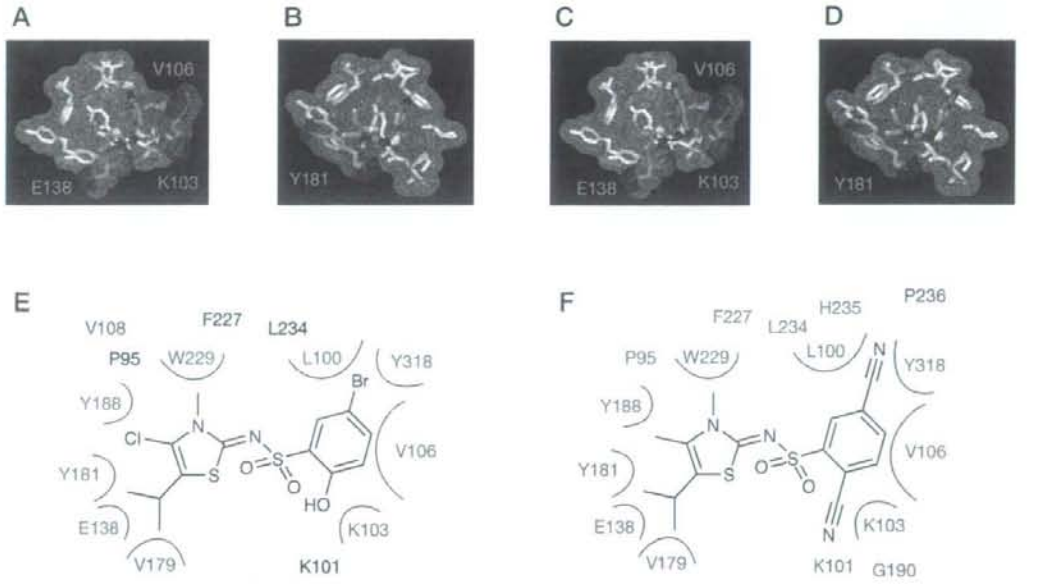

HIV type-1 (HIV-1) reverse transcriptase binding schemes (Protein Data Bank code 1HNV) [33] to **(A** & **B)** YM-215389 or **(C** & **D)** YM-228855 are shown. Blue, yellow and red indicate nitrogen, oxygen and sulfur, respectively. The K103 amino acid is indicated in orange and those of V106, E138 and Y181 are in green. Models of the interactions between the non-nucleoside reverse transcriptase inhibitor-binding hydrophobic pockets (NNRTI-BHP) and **(E)** YM-215389 and **(F)** YM-228855 are shown. The distances between YM-215389 and YM-228855 and the amino acids in the NNRTI-BHP are indicated in red (within 3.5 Å) and black (3.5–4.0 Å). V108 is indicated in blue (E) because the distance from the methyl moiety at the thiazole ring of YM-215389 is 6.8 Å.

with NNRTIs. It also stabilizes the unliganded closed conformation of the NNRTI-BHP [9,34].

For YM-215389, the effect of K103N mutation on its anti-HIV-1 activity was smaller than NVP, EFV and YM-228855 (Table 1). In fact, four amino acid substitutions were required for YM-215389 to develop strong resistance (>500-fold). Interestingly, all substituted mutants observed during HIV-$1_{YM\text{-}215389}{}^{R}$ selection increased the susceptibility to AZT. This means that the emergence of resistance to YM-215389 does not occur readily, especially when the drug is used in combination with AZT. These results suggest that YM-215389 is a valuable lead compound in the search for next generation NNRTIs. The docking study showed that YM-215389 interacts hydrophobically with multiple amino acids in NNRTI-BHP, that is, YM-215389 interacts uniformly with L100, K103, V106 and Y318 through the benzene ring, and with E138, V179, Y181, Y188 and W229 through the thiazole ring (Figures 2A, 2B & 2E). A single amino acid substitution over a large area within the NNRTI-BHP confers only moderate resistance to YM-215389 (Table 1). YM-215389 is thought to maintain its anti-HIV-1 activity to major NNRTI-resistant mutants by adjusting the hydrophobic interactions with NNRTI-BHP via a sulfonamide backbone that can be rotated intermediately. The anti-HIV-1 activity of YM-228855 (EC_{50}=2 nM) was more potent than that of YM-215389 (EC_{50}=20 nM). However, its potent anti-HIV-1 activity was strongly reduced by single amino acid substitutions (Y181I, K103N and Y181C substitutions resulted in 540-, 87- and 54-fold reductions, respectively). These results suggest that the cyano-moieties on the benzene ring of YM-228855 contribute to the enhanced anti-HIV-1 activity, but its protruding character restricts conformational adjustment with NNRTI-BHP.

The advantage of conformational adaptability has also been demonstrated with another NNRTI [39]. A diarylpyrimidine derivative, etravirine (TMC125-R165335) that inhibits various NNRTI-resistant clones with single amino acid substitutions, binds to the NNRTI-BHP using several binding modes. Cocrystallization of RT with etravirine results in resolution of only 6–8 Å (crystal grams), even when

using high-intensity synchrotron radiation, because the conformations corresponding with RT and etravirine that coexist in the crystal are different [40]. Like etravirine, YM-215389 has an intermediately rotatable sulfonamide backbone, which allows for more conformational adaptability than NVP and EFV can achieve. This is because NVP has a highly rigid dihydrodipyridodiazepine (triple ring) backbone and EFV has a relatively rigid 4-alkynyldihydrobenzoxazine-containing triple bond between its body and left wing.

It has also been reported that inhibitors carrying molecularly flexible groups tend to be able to adapt to mutated enzymes. For instance, tenofovir (9-*R*-2-phosphonomethoxypropyl adenine [PMPA]), an acyclic NRTI, inhibits various types of drug resistance to HIV-1 variants both *in vitro* and *in vivo* [41,42]. PMPA has a highly flexible acyclic sugar compared with other NRTIs, for example, 2′,3′-dideoxyinosine, which confers the advantages of NRTIs [43]. PMPA can bind even to a mutated 3′-OH binding site, for example, K65, R72, Y115 and Q151, and be incorporated into the elongating primer end to block it. The incorporated PMPA can also escape excision by ATP. Thus, PMPA effectively inhibits viral DNA synthesis mediated by RT with resistance mutations. It has also been reported that the flexible HIV-1 protease inhibitor, JE-2147, which contains a P2′ benzylamide group with two rotatable bonds, is able to inhibit various protease inhibitor-resistant variants. However, the inflexible derivative, JE-533, which contains a *t*-butylamide group with only one rotatable bond at this position, fails to suppress the resistant variants [44].

In this report, the anti-HIV-1 activities of YM-215389 and YM-228855 against various substituted variants were investigated. The data suggest that conformational adaptability of hydrophobic interactions is important for enabling NNRTIs to maintain their anti-HIV activity against various HIV-1 variants. Therefore, YM-215389 is considered to be a promising lead compound for the next generation of NNRTIs.

Acknowledgements

We would like to thank Miyuki Ino, Mieko Ikeuchi and Shuhei Taguwa for technical assistance and Ayako Yoshioka for the manuscript preparation. The HeLa-CD4-LTR/β-gal cells were kindly provided by Dr Michael Emerman through the AIDS Research and Reference Reagent Program, Division of AIDS, NIAID, NIH (Bethesda, MD, USA). The pNL101 plasmid was a kind gift from Dr Kuan-Teh Jeang (NIH). This work was supported in part by grants for the Promotion of AIDS Research from the Ministry of Health and Welfare and for the Ministry of Education, Culture, Sports, Science and Technology of Japan (EK), and a grant for Research for Health Sciences Focusing on Drug Innovation from The Japan Health Sciences Foundation (EK and MM).

Figure 3. Three-dimensional structures of YM-215389 and YM-228855

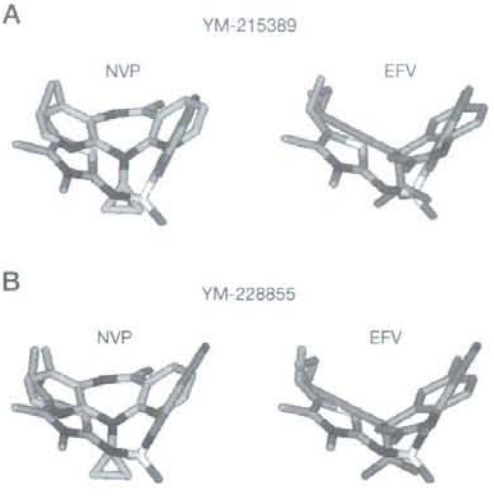

Superimposed comparisons of the three-dimensional structures of (A) YM-215389 to nevirapine (NVP) or efavirenz (EFV) and (B) YM-228855 to NVP or EFV are shown. Thiazole derivatives, NVP and EFV are indicated in gray, emerald and brown, respectively. Blue, yellow, red and green indicate nitrogen, sulfur, oxygen and fluorine, respectively.

Figure 4. Estimated flexibility of YM-215389

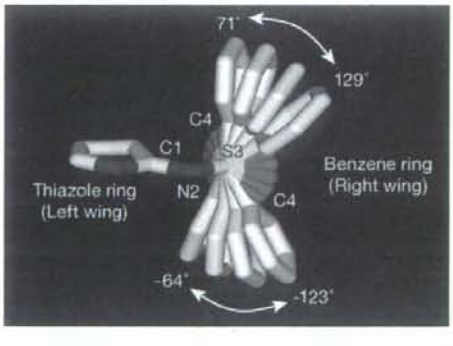

The flexibility of thiazolidenebenzenesulfonamide derivatives were estimated from 24 compounds with a thiazole ring-sulfonamide-benzene ring deposited in the Cambridge Structural Database [26]. The estimated torsion angles of C1-N2-S3-C4 are shown.